Closed-form multi-dimensional solutions and asymptotic behaviours for subdiffusive processes with crossovers: II. Accelerating case

Emad Awad[1] **and Ralf Metzler**[2,*] (ID)

[1] Department of Mathematics, Faculty of Education, Alexandria University, Souter St. El-Shatby, Alexandria PO Box 21526, Egypt
[2] Institute of Physics and Astronomy, University of Potsdam, Karl-Liebknecht-Str. 24/25, D-14476 Potsdam-Golm, Germany

E-mail: emadawad78@alexu.edu.eg and rmetzler@uni-potsdam.de

CrossMark

Abstract

Anomalous diffusion with a power-law time dependence $\langle |\mathbf{R}|^2(t) \rangle \simeq t^{\alpha_i}$ of the mean squared displacement occurs quite ubiquitously in numerous complex systems. Often, this anomalous diffusion is characterised by crossovers between regimes with different anomalous diffusion exponents α_i. Here we consider the case when such a crossover occurs from a first regime with α_1 to a second regime with α_2 such that $\alpha_2 > \alpha_1$, i.e., accelerating anomalous diffusion. A widely used framework to describe such crossovers in a one-dimensional setting is the bi-fractional diffusion equation of the so-called modified type, involving two time-fractional derivatives defined in the Riemann–Liouville sense. We here generalise this bi-fractional diffusion equation to higher dimensions and derive its multidimensional propagator (Green's function) for the general case when also a space fractional derivative is present, taking into consideration long-ranged jumps (Lévy flights). We derive the asymptotic behaviours for this propagator in both the short- and long-time as well the short- and long-distance regimes. Finally, we also calculate the mean squared displacement, skewness and kurtosis in all dimensions, demonstrating that in the general case the non-Gaussian shape of the probability density function changes.

*Author to whom any correspondence should be addressed.

(Some figures may appear in colour only in the online journal)

1. Introduction

Robert Brown's lucid account on the jittery motion of microscopic particles almost two centuries ago [1] paved the way for one of the most outstanding scientific developments, the history of diffusion. Following the seminal theoretical works by Albert Einstein [2], Marian Smoluchowski [3], William Sutherland [4], and Paul Langevin [5], Brownian motion is described as the thermally driven, effectively random motion of a passive tracer particle. On a more general level, stochastic processes have been ever more widely applied in the sciences [6–8] and have also become a focus field in mathematics [9–11]. The chief characteristics of 'Brownian motion', 'normal diffusion', or 'Gaussian diffusion' are the linear time dependence $\langle|\mathbf{R}|^2(t)\rangle \propto t$ of the mean squared displacement (MSD) and the Gaussian shape $W(\mathbf{R}, t) = (4\pi Dt)^{-d/2} \exp(-|\mathbf{R}|^2/[4Dt])$ of the probability density function (PDF, also called propagator or Green's function) for a point-like initial condition [7, 12]. We note that the occurrence of a linear time dependence of the MSD is not sufficient to define Brownian motion, as underlined by the growing number of systems exhibiting a linear MSD but pronouncedly non-Gaussian displacement distributions [13–18].

Based on his study of the random spreading of two pilot balloons relative to each other, Lewis Fry Richardson reported the cubic scaling $\langle|\mathbf{R}|^2(t)\rangle \propto t^3$ of the MSD [19]. This was likely the first report of what we nowadays refer to as 'anomalous diffusion', a phenomenon typically connected with the power-law form [20, 21]

$$\langle|\mathbf{R}|^2(t)\rangle \propto t^\alpha \tag{1}$$

of the MSD, in which $\alpha \neq 1$. For $\alpha > 1$, as in Richardson's work, we call the process superdiffusive, while for $0 < \alpha < 1$ we speak of subdiffusion. A classical example for the latter is diffusion on geometric fractals, in which the anomalous diffusion exponent was conjectured to be $\alpha = 2/(2 + \overline{\delta})$ with $\overline{\delta} > 0$ by Shlomo Alexander and Ray Orbach [22]. By now a vast number of studies have reported anomalous diffusion of the form (1), ranging from stochastic motion in biological cells [23, 24] to geophysical contexts [25, 26].

Often, systems exhibit crossover behaviours at some characteristic time scales. We are here interested in crossovers of the form

$$\langle|\mathbf{R}|^2(t)\rangle \simeq \begin{cases} t^{\alpha_1}, & t \to 0^+ \\ t^{\alpha_2}, & t \to \infty \end{cases} \tag{2}$$

showing two distinct power-law regimes with scaling exponents α_1 and α_2. In reality, the system of interest may show additional regimes at times shorter than some microscopic time scale, or longer than some macroscopic correlation time reflecting, e.g., the finite system size. In the mathematical framework we have in mind here, we treat systems with an observed crossover between two power-laws as indicated in equation (2). In what follows we consider the accelerating case when $\alpha_2 > \alpha_1$, the opposite, retarding case was recently considered by us [67].

A prototypical example is the motion of lipid molecules in bilayer membranes studied by supercomputing approaches [27] or by neutron spin echo methods [28]. Depending on the exact

composition or physical phase of the bilayer, crossovers may occur from a subdiffusive regime with $0 < \alpha_1 < 1$ to a normal diffusive regime with $\alpha_2 = 1$ or another yet faster subdiffusive regime with $0 < \alpha_1 < \alpha_2 < 1$ [27, 28]. One of these crossovers occurs at time scales of some 10 ns, typically associated with the loss of correlations of a single lipid molecule [29, 30]. Similar accelerating crossovers are seen in the diffusion dynamics of proteins [31] or surface water [32, 33] along membrane surfaces, or for surface water of proteins [34]. In non-inert obstacle environments crossovers from slower to faster passive diffusion occurs for specific parameter combinations [35]. Crossover behaviours are also observed in simulations of the lateral motion of drug molecules in a silica slab [36]. Moreover, in active matter crossovers from a short-time passive viscoelastic-like subdiffusive behaviour to a superdiffusive regime at longer times are observed for the motion of microscopic vesicles in amoeba cells [37–39]. The choice of specific models for the description of the observed crossover dynamics depends on the exact physical situation.

Different scenarios for crossover behaviours occur when $\alpha_2 = 0$ indicates the occurrence of a plateau, typically due to confinement, see, e.g., [40, 41]. Another scenario is observed for caging-like effects, when an initial power-law with scaling exponent α_1 is interrupted by a slow-down, extended crossover regime, that finally crosses over to a second power-law regime with exponent α_2, see, e.g., [41–44]. We note that crossovers analogous to those discussed here may also be observed in the power spectra, see, e.g., the discussion in [39, 45]. Finally, we also note that apparent acceleration may also be caused by positional noise [46].

One way to generalise the standard diffusion equation encoding the linear growth (1) of the MSD with $\alpha = 1$ for situations with non-linear growth (i.e., $\alpha \neq 1$) is to introduce a position and time dependent diffusion coefficient, $k(\mathbf{R}, t)$, obtaining the generalised diffusion equation [47, 48]

$$\frac{\partial \Omega^{(n)}(\mathbf{R}, t)}{\partial t} = \nabla_{\mathbf{R}} \cdot \left[k(\mathbf{R}, t) \nabla_{\mathbf{R}} \Omega^{(n)}(\mathbf{R}, t) \right], \tag{3}$$

where $\Omega^{(n)}(\mathbf{R}, t)$ is the multidimensional PDF or propagator, $\mathbf{R} = (X_1, X_2, \ldots, X_n) \in \mathbb{R}^n$ the position vector, t denotes time, and $\nabla_{\mathbf{R}} \cdot$ is the divergence operator. With the specific choice $k(\mathbf{R}, t) = C_0 D R^{4/3}$ ($R = |\mathbf{R}|$), where D is the diffusivity constant and C_0 is a constant to keep dimensions in order, Richardson [19] obtained the cubic scaling of the MSD with $\alpha = 3$. Batchelor obtained the same MSD scaling with a t^2-dependent form of the generalised diffusion coefficient [49]. Another alternative kinetic approach to obtain the Richardson's cubic scaling is to replace (3) with

$$\frac{\partial^3 \Omega^{(n)}(\mathbf{R}, t)}{\partial t^3} = C_1 D \Delta_{\mathbf{R}} \Omega^{(n)}(\mathbf{R}, t), \tag{4}$$

where C_1 is a dimensional constant and $\Delta_{\mathbf{R}}$ the Laplace operator [47, 48]. Such equations with a time derivative of order different from unity were generalised in terms of different fractional derivatives [21]. Notably Schneider and Wyss introduced a fractional diffusion-wave equation for the description of anomalous diffusion characterised by the MSD (1) with $0 < \alpha < 2$ and presented the solution in terms of Fox H-functions [57]. Today, both time and space fractional diffusion equations are used in various forms, see, e.g., [21, 50–56].

Crossover behaviours between different diffusion regimes have also been addressed in terms of fractional dynamic equations. Thus a crossover from superdiffusion to subdiffusion was found to be captured through a generalised Cattaneo (telegrapher's) equation [58]. Retarding and accelerating crossovers (2) were found to be mathematically described via replacing the

fractional derivative of fixed order in the fractional diffusion equation with another of distributed order [59–65]. Recently, it was shown that the generalised Jeffreys equation, with flux-driven description, captures a crossover caging-like effect [66].

Here we further pursue the concept of distributed order fractional equations to determine the detailed properties in higher dimensions. In [67] we previously considered the bi-fractional diffusion equation of the natural type in n dimensions and derived the propagator and the asymptotic dynamic behaviours. In this work we continue our study and consider the accelerating case. The paper is organised as follows: in section 2 we consider the bi-fractional diffusion equation of the modified type with additional space-fractional operator in n dimensions and derive the multidimensional propagator. We prove the non-negativity of this propagator in higher dimensions in section 3. In section 4 we derive the asymptotic behaviours for these accelerating processes in the short-time and long-time regimes. Moreover we determine the moments as function of time in section 5 and show explicit solutions for the skewness and the kurtosis in all dimensions. Finally we draw our conclusion in section 6.

2. Fractional kinetic equations and solutions

2.1. Bi-fractional diffusion equation

The fractional diffusion equation of the modified type, in dimensionless form, in n-dimensional Euclidean space $\mathbb{R}^n$ reads [21, 57, 67]

$$\frac{\partial W^{(n)}(\mathbf{r}, t)}{\partial t} = {}_0^{\mathrm{RL}}\mathcal{D}_t^{1-\alpha} \Delta W^{(n)}(\mathbf{r}, t), \tag{5}$$

where $0 < \alpha < 1$, $W^{(n)}(\mathbf{r}, t)$ is the n-dimensional propagator ($n = 1$, 2, and 3), $\mathbf{r} = (x_1, \ldots, x_n) \in \mathbb{R}^n$ is the dimensionless position vector, t the dimensionless time, Δ the fractional Laplace operator, and ${}_0^{\mathrm{RL}}\mathcal{D}_t^{\alpha}$ is the Riemann–Liouville fractional derivative of order $\alpha \in (0, 1]$, defined for any generic function $f(t)$ as [68]

$$
{}_0^{\mathrm{RL}}\mathcal{D}_t^{\alpha} f(t) = \begin{cases} \dfrac{1}{\Gamma(1-\alpha)} \dfrac{\mathrm{d}}{\mathrm{d}t} \displaystyle\int_0^t \dfrac{f(\zeta)}{(t-\zeta)^{\alpha}} \, \mathrm{d}\zeta, & 0 < \alpha < 1 \\ \dfrac{\mathrm{d}f(t)}{\mathrm{d}t}, & \alpha = 1. \end{cases} \tag{6}
$$

When $\alpha = 1$, equation (5) reduces to the normal diffusion equation in n-dimensional space with the Gaussian propagator

$$W^{(n)}(\mathbf{r}, t) = G^{(n)}(\mathbf{r}, t) = \frac{1}{(4\pi t)^{n/2}} \exp\left(-\frac{|\mathbf{r}|^2}{4t}\right). \tag{7}$$

We note that the fractional diffusion equation (5) can be derived from the continuous-time random walk model with a scale-free waiting time PDF of asymptotic power-law form $\simeq t^{-1-\alpha}$ with $0 < \alpha < 1$ [21, 69–74].

Let us now consider a generalisation of equation (5) with distributed-order fractional derivative [61–65], in n-dimensional space,

$$\frac{\partial W^{(n)}(\mathbf{r}, t)}{\partial t} = -\int_0^1 p(\nu) {}_0^{\mathrm{RL}}\mathcal{D}_t^{1-\nu} (-\Delta)^{\mu/2} W^{(n)}(\mathbf{r}, t) \mathrm{d}\nu, \tag{8}$$

where $p(\nu)$ is a PDF in the sense that $p(\nu) \geqslant 0$ and $\int_0^1 p(\nu)\mathrm{d}\nu = 1$. Here we also accommodated the space-fractional derivative $-(-\Delta)^{\mu/2}$ instead of the ordinary Laplacian Δ, in order to be

able to include long-tailed jump lengths in our formalism [21]. The space-fractional derivative is defined for a generic function $f^{(n)} : \mathbb{R}^n \to \mathbb{R}$ as a pseudo-differential operator characterised by its Fourier transform via [75–78]

$$\mathscr{F}_n\left\{(-\Delta)^{\mu/2}f^{(n)}(\mathbf{r})\right\}(\mathbf{q}) = \int_{\mathbb{R}^n}(-\Delta)^{\mu/2}f^{(n)}(\mathbf{r})\exp(\imath\mathbf{q}\cdot\mathbf{r})\mathrm{d}^n\mathbf{r}$$

$$= |\mathbf{q}|^\mu \mathscr{F}_n\left\{f^{(n)}(\mathbf{r})\right\}(\mathbf{q}), \tag{9}$$

where $1 < \mu < 2$.[3] In the limit $\mu = 2$ we return to the standard Laplacian. This fractional order in space specifically turns out to be useful in handling the divergent two-dimensional solution, as shown in [67]. In the particular case

$$p(\nu) = p_1\delta(\nu - \alpha_1) + p_2\delta(\nu - \alpha_2), \tag{10}$$

where p_1 and p_2 are positive constants satisfying $p_1 + p_2 = 1$ and $0 < \alpha_1 < \alpha_2 \leqslant 1$, equation (8) reduces to

$$\frac{\partial W^{(n)}(\mathbf{r},t)}{\partial t} = -\left(p_1{}_0^{\mathrm{RL}}\mathcal{D}_t^{1-\alpha_1} + p_2{}_0^{\mathrm{RL}}\mathcal{D}_t^{1-\alpha_2}\right)(-\Delta)^{\mu/2}W^{(n)}(\mathbf{r},t). \tag{11}$$

Equation (11) is called the bi-fractional diffusion equation (in time) of modified type with an additional space-fractional operator. It was shown that the MSD governed by equation (11), with $\mu = 2$, in the one-dimensional setting exhibits an accelerating subdiffusive crossover (2) with $0 < \alpha_1 < \alpha_2 \leqslant 1$, i.e., the smaller exponent dominates the short-time regime while the larger exponent controls the long-time regime. In what follows we consider the solution of the initial value problem consisting of equation (11) subject to the point-like initial condition

$$W^{(n)}(\mathbf{r},0^+) = \delta(\mathbf{r}), \tag{12}$$

where $\delta(\cdot)$ is the multidimensional Dirac delta function.

2.2. Multidimensional propagator

We proceed to derive a closed-form expression for the multidimensional propagator for the generalised diffusion equation (11) subject to the initial condition (12). Let us first write the propagator $W^{(n)}(\mathbf{r},t)$ in Fourier–Laplace space [79] as

$$\widehat{\widetilde{W}}^{(n)}\left(|\mathbf{q}|,s\right) = \frac{s^{\alpha_1-1}}{s^{\alpha_1} + p_1|\mathbf{q}|^\mu}\left(1 + \frac{p_2 s^{\alpha_1-\alpha_2}|\mathbf{q}|^\mu}{s^{\alpha_1} + p_1|\mathbf{q}|^\mu}\right)^{-1}, \tag{13}$$

where the tilde refers to the Laplace transform $\widetilde{f}(\mathbf{r},s) = \mathscr{L}\{f(\mathbf{r},t);t\}(\mathbf{r},s) = \int_0^\infty f(\mathbf{r},t)\exp(-st)\mathrm{d}t$, the hat refers to the Fourier transform $\widehat{f}(q,t) = \mathscr{F}_n\{f^{(n)}(\mathbf{r},t)\}(\mathbf{q},t) = \int_{\mathbb{R}^n}f^{(n)}(\mathbf{r},t)\exp(\imath\mathbf{q}\cdot\mathbf{r})\mathrm{d}^n\mathbf{r}$, $s \in \mathbb{C}$ is the Laplace variable, and $\mathbf{q} = (q_1, \ldots, q_n) \in \mathbb{R}^n$ is the wave vector, $|\mathbf{q}|^2 = q_1^2 + \cdots + q_n^2$ and $n = 1, 2$ or 3. Equation (13) can be written in the form [80]

$$\widehat{\widetilde{W}}^{(n)}(|\mathbf{q}|,s) = \sum_{k=0}^\infty (-p_2|\mathbf{q}|^\mu)^k \frac{s^{(\alpha_1-\alpha_2)k+\alpha_1-1}}{\left(s^{\alpha_1} + p_1|\mathbf{q}|^\mu\right)^{k+1}}. \tag{14}$$

The condition $|x| < 1$ to apply the negative binomial series $(1 + x)^{-1} = \sum_{k=0}^\infty(-x)^k$ in this transformation is fulfiled when the condition $|\mathbf{q}| \ll s^{(\alpha_2-\alpha_1)/\mu}$ holds. This corresponds to

---

[3] We do not consider the case $0 < \mu \leqslant 1$ in this work.

the known correct diffusion limit that taking $|\mathbf{q}| \to 0$ precedes the limit $s \to 0$ [81]. From a numerical point of view, for finite values of the variables care should be taken that the fraction $p_2 s^{\alpha_1 - \alpha_2} |\mathbf{q}|^{\mu} / \left(s^{\alpha_1} + p_1 |\mathbf{q}|^{\mu} \right)$ does not exceed unity. Inverting the Laplace transform in equation (14), utilising relation (A17), we obtain

$$\widehat{W}^{(n)}(|\mathbf{q}|, t) = \sum_{k=0}^{\infty} (-p_2 t^{\alpha_2} |\mathbf{q}|^{\mu})^k E_{\alpha_1, \alpha_2 k+1}^{k+1}(-p_1 t^{\alpha_1} |\mathbf{q}|^{\mu}), \tag{15}$$

where $E_{\alpha,\beta}^{\gamma}(\cdot)$ is the generalised Mittag–Leffler function with three parameters, see appendix A. Next, we invert the Fourier transform to obtain

$$W^{(n)}(\mathbf{r}, t) = \left(\frac{1}{2\pi} \right)^n \sum_{k=0}^{\infty} (-p_2 t^{\alpha_2})^k$$
$$\times \int_{\mathbb{R}^n} \exp(-\imath \mathbf{q} \cdot \mathbf{r}) |\mathbf{q}|^{\mu k} E_{\alpha_1, \alpha_2 k+1}^{k+1} \left(-p_1 t^{\alpha_1} |\mathbf{q}|^{\mu} \right) d^n \mathbf{q}. \tag{16}$$

Due to the symmetry $\widehat{W}^{(n)}(\mathbf{q}, t) = \widehat{W}^{(n)} \left(|\mathbf{q}|, t \right) = \widehat{W}^{(n)}(q, t)$, where $q = |\mathbf{q}|$, we can write

$$W^{(n)}(\mathbf{r}, t) = \left(\frac{1}{2\pi} \right)^n \int_{\mathbb{R}^n} \exp(-\imath \mathbf{q} \cdot \mathbf{r}) \widehat{W} \left(|\mathbf{q}|, t \right) d^n \mathbf{q}$$
$$= \frac{r^{1-\frac{n}{2}}}{(2\pi)^{\frac{n}{2}}} \int_0^{\infty} J_{\frac{n-2}{2}}(qr) q^{\frac{n}{2}} \widehat{W}(q, t) dq, \tag{17}$$

where J_{ν} denotes the Bessel function of the first kind of order ν. Therefore, we arrive at

$$W^{(n)}(\mathbf{r}, t) = \frac{r^{1-\frac{n}{2}}}{(2\pi)^{\frac{n}{2}}} \sum_{k=0}^{\infty} (-p_2 t^{\alpha_2})^k$$
$$\times \int_0^{\infty} q^{\frac{n}{2} + \mu k} J_{\frac{n-2}{2}}(qr) E_{\alpha_1, \alpha_2 k+1}^{k+1} \left(-p_1 t^{\alpha_1} q^{\mu} \right) dq. \tag{18}$$

The integral in the sum of equation (18) is the Hankel transform of the generalised Mittag–Leffler function given by (A18), see [67, 82]. Thus, we have a closed-form solution of the multidimensional propagator of the bi-fractional diffusion equation of modified type with space fractality (11) subject to (12), in the form

$$W^{(n)}(\mathbf{r}, t) = \left(\frac{1}{2^{\mu} \pi^{\frac{\mu}{2}} p_1 t^{\alpha_1}} \right)^{\frac{n}{\mu}} \sum_{k=0}^{\infty} \frac{(-1)^k}{k!} \left(\frac{p_2}{p_1} t^{\alpha_2 - \alpha_1} \right)^k$$
$$\times H_{2,3}^{2,1} \left[\frac{r^{\mu}}{2^{\mu} p_1 t^{\alpha_1}} \left| \begin{array}{c} \left(1 - k - \frac{n}{\mu}, 1 \right); \left(1 - \frac{n\alpha_1}{\mu} + (\alpha_2 - \alpha_1)k, \alpha_1 \right) \\ \left(0, \frac{\mu}{2} \right), \left(1 - \frac{n}{\mu}, 1 \right); \left(1 - \frac{n}{2}, \frac{\mu}{2} \right) \end{array} \right. \right], \tag{19}$$

with the condition $p_1 > p_2$ to ensure convergence of the solution for long times. Here, $H_{p,q}^{m,n}(\cdot)$ is the Fox H-function, see appendix A. As it should, when $\mu = 2$ and $n = 1$, we get exactly the one-dimensional solution of the bi-fractional diffusion equation of the modified type without space fractality, as obtained in [79]. Note that to obtain numerical results we utilise the expansion (A5) of the H-function.

3. Non-negativity in higher dimensions

In this section we show that the one-, two-, and three-dimensional solutions of the bi-fractional diffusion equation of the modified type without space fractality, i.e., equation (11) with $\mu = 2$, are non-negative. To achieve this objective, we follow two different methods: the first depends on writing these solutions in Laplace space and examining whether these solutions are completely monotone functions if confined to the positive real line or not, while the second approach is to test whether the multidimensional propagator $W^{(n)}(\mathbf{r}, t)$ is subordinated to the Wiener process or not.

Introducing the parameter $\lambda = \Re\{s\}$, which represents the positive real part of the Laplace variable, and rewriting the one-, two-, and three-dimensional solutions in equation (11) with $\mu = 2$ in terms of λ, in Laplace domain we find [83]

$$\widetilde{W}^{(1)}(x, \lambda) = \frac{1}{2\lambda\sqrt{p_1\lambda^{-\alpha_1} + p_2\lambda^{-\alpha_2}}} \exp\left(-\frac{|x|}{\sqrt{p_1\lambda^{-\alpha_1} + p_2\lambda^{-\alpha_2}}}\right), \qquad (20)$$

$$\widetilde{W}^{(2)}(r, \lambda) = \frac{1}{2\pi\lambda(p_1\lambda^{-\alpha_1} + p_2\lambda^{-\alpha_2})} K_0\left(\frac{r}{\sqrt{p_1\lambda^{-\alpha_1} + p_2\lambda^{-\alpha_2}}}\right), \qquad (21)$$

$$\widetilde{W}^{(3)}(r, \lambda) = \frac{1}{4\pi r\lambda(p_1\lambda^{-\alpha_1} + p_2\lambda^{-\alpha_2})} \exp\left(-\frac{r}{\sqrt{p_1\lambda^{-\alpha_1} + p_2\lambda^{-\alpha_2}}}\right), \qquad (22)$$

where $K_\nu(\cdot)$ is the modified Bessel function of the second kind of order ν.

Based on the fact that the function $f(t)$ is non-negative if its Laplace transform defined on the positive real line, i.e., $\widetilde{f}(\lambda)$, is a completely monotone function (CMF) [84, 85], we can prove the non-negativity of the solutions $W^{(n)}(\cdot, t)$, $n = 1, 2, 3$, by showing that their Laplace transform (20)–(22) defined on the positive real line are CMFs.

We know that the function $\lambda^{-\alpha}$, where $\lambda > 0$ and $\alpha \in (0, 1)$, is a Stieltjes function (SF) [11], then the functions $\lambda^{-\alpha_1}$ and $\lambda^{-\alpha_2}$ are also SFs for $\lambda > 0$ and $0 < \alpha_1 < \alpha_2 < 1$. Since any linear combination of SFs is also a SF, therefore the combination $(p_1\lambda^{-\alpha_1} + p_2\lambda^{-\alpha_2})$ is a SF. Also, since for any SF, $\widetilde{f}(\lambda) \in$ SF, its square root is a SF, i.e., $\sqrt{\widetilde{f}(\lambda)} \in$ SF, then $\sqrt{p_1\lambda^{-\alpha_1} + p_2\lambda^{-\alpha_2}}$ is a SF. Furthermore, since the function $1/\widetilde{f}(\lambda)$ is a complete Bernstein function (CBF), which is a subset of the Bernstein functions (BFs) [11], if and only if $\widetilde{f}(\lambda)$ is a SF, one therefore deduces that

$$\frac{1}{p_1\lambda^{-\alpha_1} + p_2\lambda^{-\alpha_2}}, \quad \frac{1}{\sqrt{p_1\lambda^{-\alpha_1} + p_2\lambda^{-\alpha_2}}} \in \text{CBF}. \qquad (23)$$

Using the property that $\widetilde{\varphi}(\lambda)/\lambda$ is CMF if $\widetilde{\varphi}(\lambda)$ is BF, then we can write

$$\frac{1}{\lambda(p_1\lambda^{-\alpha_1} + p_2\lambda^{-\alpha_2})}, \quad \frac{1}{\lambda\sqrt{p_1\lambda^{-\alpha_1} + p_2\lambda^{-\alpha_2}}} \in \text{CMF}. \qquad (24)$$

Conversely, we know that the functions $\exp(-a\lambda)$ and $K_0(a\lambda)$ are CMF [83], and any CMF of the BF is also a CMF, i.e., if $\widetilde{\psi}_1(\lambda) \in$ CMF and $\widetilde{\psi}_2(\lambda) \in$ BF, then $\widetilde{\psi}_1\left(\widetilde{\psi}_2(\lambda)\right) \in$ CMF. Therefore, one has

$$\exp\left(-\frac{r}{\sqrt{p_1\lambda^{-\alpha_1} + p_2\lambda^{-\alpha_2}}}\right), \quad K_0\left(\frac{r}{\sqrt{p_1\lambda^{-\alpha_1} + p_2\lambda^{-\alpha_2}}}\right) \in \text{CMF}. \qquad (25)$$

In view of relations (24) and (25), the functions $\widetilde{W}^{(n)}(\cdot, \lambda)$ in equations (20)–(22) are CMFs, as products of two CMFs. This shows that the solutions $W^{(n)}(\cdot, t)$, are non-negative functions for $0 < \alpha_1 < \alpha_2 < 1$, $p_1, p_2 > 0$, and $r \geqslant 0$.

The second approach usually used to show the non-negativity of the solutions is based on the concept of subordination [84] according to which the solution of the governing equation is written as a transformation of the Gaussian distribution, namely,

$$W^{(n)}(r, t) = \int_0^\infty N(u, t) G^{(n)}(r, u) \mathrm{d}u, \tag{26}$$

where $G^{(n)}(r, t)$ is the Gaussian distribution in the n-dimensional Euclidean space defined through equation (7). Showing that $N(u, t)$ is a non-negative function for $t > 0$ and $u > 0$, one can thus infer that $W^{(n)}(r, t)$ is non-negative. This approach was successfully employed to demonstrate the non-negativity in the one-dimensional setting [61, 86]. Here, we show its validity in higher dimensions. Let us write the propagator (11) of the bi-fractional diffusion equation (11) in Laplace–Fourier space as

$$\widehat{\widetilde{W}}^{(n)}\left(|\mathbf{q}|, s\right) = \frac{a^2(s)/s}{a^2(s) + |\mathbf{q}|^2}, \qquad a^2(s) = \frac{1}{p_1 s^{-\alpha_1} + p_2 s^{-\alpha_2}}. \tag{27}$$

Using the relation $\zeta^{-1} = \int_0^\infty \exp(-u\zeta)\mathrm{d}u$ [87], equation (27) can be written as

$$\widehat{\widetilde{W}}^{(n)}\left(|\mathbf{q}|, s\right) = \int_0^\infty \left(\frac{a^2(s)}{s} \exp\left(-a^2(s)u\right)\right) \exp\left(-|\mathbf{q}|^2 u\right) \mathrm{d}u. \tag{28}$$

Inverting the Fourier transform, we have that $G^{(n)}(r, u) = \mathscr{F}_n^{-1}\left\{\exp\left(-|\mathbf{q}|^2 u\right)\right\}$, and therefore

$$\widetilde{W}^{(n)}(r, s) = \int_0^\infty \widetilde{N}(u, s) G^{(n)}(r, u) \mathrm{d}u, \tag{29}$$

where

$$\widetilde{N}(u, s) = \frac{1}{s\left(p_1 s^{-\alpha_1} + p_2 s^{-\alpha_2}\right)} \exp\left(-\frac{u}{p_1 s^{-\alpha_1} + p_2 s^{-\alpha_2}}\right). \tag{30}$$

From the discussion of relations (24) and (25), one can show that $\widetilde{N}(u, \lambda)$ is a CMF as a product of two CMFs. This proves the non-negativity of $N(u, t)$ for $u > 0$ and $t > 0$, which in turn proves the non-negativity of $W^{(n)}(r, t)$.

4. Asymptotic behaviours

We now derive the main results of this work, the asymptotic behaviours for the propagator (19) in the long-time domain and/or near the origin, $r^2 \ll 4p_1 t^{\alpha_1}$, and in the short-time domain and/or far from the origin, $r^2 \gg p_1 t^{\alpha_1}$.

4.1. Behaviour at long times and/or near the origin

We use the general asymptotic behaviour (A6) of the H-function for small argument and its expansion (A3) to derive asymptotic expressions for the H-function (A5) in the n-dimensional case, see equations (A8)–(A10). We utilise these relations here to obtain explicit expressions for the propagator (19) in the limit $r^2 \ll p_1 t^{\alpha_1}$.
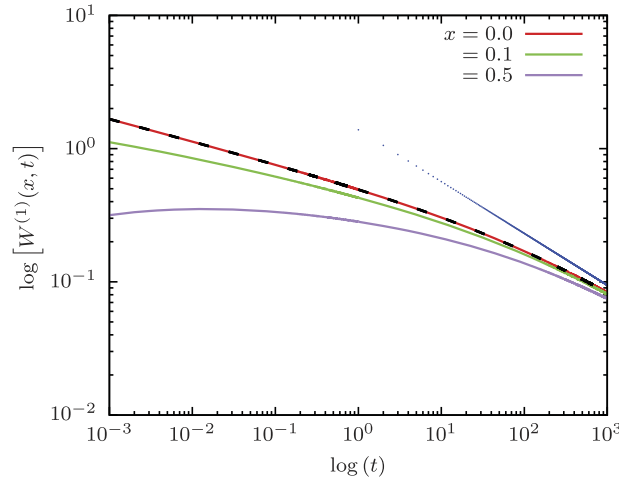
Figure 1. Evolution of the asymptotic behaviour (33) (dashed black line) and the one-dimensional propagator (31) (coloured solid curves) along the time-scale and at different values of the position variable, $x = 0$, 0.1, and 0.5. The dotted blue line shows the long-time behaviour (34) near the origin. The model parameters are chosen as $p_1 = 0.9$, $p_2 = 0.1$, $\alpha_1 = 0.3$, $\alpha_2 = 0.7$, and $\mu = 1.8$ (fractional Laplacian operator).

4.1.1. 1D case. The 1D solution of the dynamic equation (11), given by the choice $n = 1$ in result (19), reads

$$
W^{(1)}(x,t) = \frac{1}{2}\sqrt{\pi}(p_1 t^{\alpha_1})^{1/\mu} \sum_{k=0}^{\infty} \frac{(-1)^k}{k!} \left(\frac{p_2}{p_1} t^{\alpha_2 - \alpha_1} \right)^k
$$

$$
\times H_{2,3}^{2,1} \left[\frac{|x|^{\mu}}{2^{\mu} p_1 t^{\alpha_1}} \left| \begin{array}{c} \left(1 - k - \frac{1}{\mu}, 1 \right); \left(1 - \frac{\alpha_1}{\mu} + (\alpha_2 - \alpha_1)k, \alpha_1 \right) \\ \left(0, \frac{\mu}{2} \right), \left(1 - \frac{1}{\mu}, 1 \right); \left(\frac{1}{2}, \frac{\mu}{2} \right) \end{array} \right].
$$

(31)

For sufficiently long times t and small values of the distance x, i.e., $|x|^{\mu} \ll 2^{\mu} p_1 t^{\alpha_1}$, the asymptotic behaviour of the H-function in equation (31) is given by (A8), yielding the asymptotic scaling

$$
W^{(1)}(x,t) \sim \frac{\Gamma\left(1 - \frac{1}{\mu}\right)}{\mu \pi (p_1 t^{\alpha_1})^{\frac{1}{\mu}}} \sum_{k=0}^{\infty} \frac{\Gamma\left(k + \frac{1}{\mu}\right)}{\Gamma\left(1 - \frac{\alpha_1}{\mu} + (\alpha_2 - \alpha_1)k\right)} \frac{\left(-\frac{p_2}{p_1} t^{\alpha_2 - \alpha_1}\right)^k}{k!},
$$

$$
|x|^{\mu} \ll 2^{\mu} p_1 t^{\alpha_1}.
$$

(32)

Using the relation $\Gamma\left(k + \frac{1}{\mu}\right) = \left(\frac{1}{\mu}\right)_k \Gamma\left(\frac{1}{\mu}\right)$, where $\left(\frac{1}{\mu}\right)_k$ is the ascending Pochhammer symbol defined in appendix A, and the definition of the generalised Mittag–Leffler function (A14), the asymptotic behaviour (32) of the 1D solution can be rewritten in the form

$$W^{(1)}(x,t) \sim \frac{1}{\mu(p_1 t^{\alpha_1})^{\frac{1}{\mu}} \sin\left(\frac{\pi}{\mu}\right)} E^{\frac{1}{\mu}}_{\alpha_2 - \alpha_1, 1 - \frac{\alpha_1}{\mu}}\left(-\frac{p_2}{p_1} t^{\alpha_2 - \alpha_1}\right),$$

$$|x|^{\mu} \ll 2^{\mu} p_1 t^{\alpha_1}, \tag{33}$$

where $1 < \mu \leqslant 2$ and Euler's reflection formula for the Γ-function has been used. Moreover, at sufficiently long times, the leading asymptotic behaviour can be approximated by using (A15) to obtain the explicit formula

$$W^{(1)}(x,t) \sim \frac{1}{\mu p_2^{1/\mu} \sin(\pi/\mu)} \frac{t^{-\alpha_2/\mu}}{\Gamma(1 - \alpha_2/\mu)}, \quad t \to \infty, \ |x| \to 0. \tag{34}$$

In figure 1, we compare between the asymptotic behaviour (33) represented by the Mittag–Leffler function and the one-dimensional propagator (31) at different positions. Notably, one sees that the asymptotic behaviour (33) coincides well with the one-dimensional propagator at $x = 0$, along the whole time-domain. As the spatial variable increases, $x = 0.1, 0.5$, the asymptotic behaviour works only in the long-time domain. The long-time behaviour (34) near the origin is also shown.

4.1.2. 2D case.　The 2D solution of the bi-fractional diffusion equation (11), $n = 2$ in result (19), is

$$W^{(2)}(r,t) = \frac{1}{4\pi(p_1 t^{\alpha_1})^{2/\mu}} \sum_{k=0}^{\infty} \frac{(-1)^k}{k!}\left(\frac{p_2}{p_1} t^{\alpha_2 - \alpha_1}\right)^k$$

$$\times H^{2,1}_{2,3}\left[\frac{r^{\mu}}{2^{\mu} p_1 t^{\alpha_1}} \left| \begin{array}{c} \left(1 - k - \frac{2}{\mu}, 1\right); \left(1 - \frac{2\alpha_1}{\mu} + (\alpha_2 - \alpha_1)k, \alpha_1\right) \\ \left(0, \frac{\mu}{2}\right), \left(1 - \frac{2}{\mu}, 1\right); \left(0, \frac{\mu}{2}\right) \end{array}\right.\right]. \tag{35}$$

With the asymptotic behaviour (A9) of the H-function we can approximate the 2D solution (35) for $r^{\mu} \ll 2^{\mu} p_1 t^{\alpha_1}$, yielding

$$W^{(2)}(r,t) \sim \frac{1}{4\pi(p_1 t^{\alpha_1})^{2/\mu}} \left\{ \frac{2}{\mu}\Gamma\left(1 - \frac{2}{\mu}\right)\Gamma\left(\frac{2}{\mu}\right) \right.$$

$$\times \sum_{k=0}^{\infty} \frac{\left(\frac{2}{\mu}\right)_k}{\Gamma\left(1 - \frac{2\alpha_1}{\mu} + (\alpha_2 - \alpha_1)k\right)} \frac{\left(-\frac{p_2}{p_1} t^{\alpha_2 - \alpha_1}\right)^k}{k!}$$

$$\left. + \frac{\Gamma\left(1 - \frac{\mu}{2}\right)}{\Gamma\left(\frac{\mu}{2}\right)}\left(\frac{r^{\mu}}{2^{\mu} p_1 t^{\alpha_1}}\right)^{1 - \frac{2}{\mu}} \sum_{k=0}^{\infty} \frac{\left(-\frac{p_2}{p_1} t^{\alpha_2 - \alpha_1}\right)^k}{\Gamma\left(1 - \alpha_1 + (\alpha_2 - \alpha_1)k\right)} \right\},$$

$$r^{\mu} \ll 2^{\mu} p_1 t^{\alpha_1}. \tag{36}$$

Using relations (A14) and (A19) we can again invoke the generalised Mittag–Leffler function and rewrite this asymptotic form as
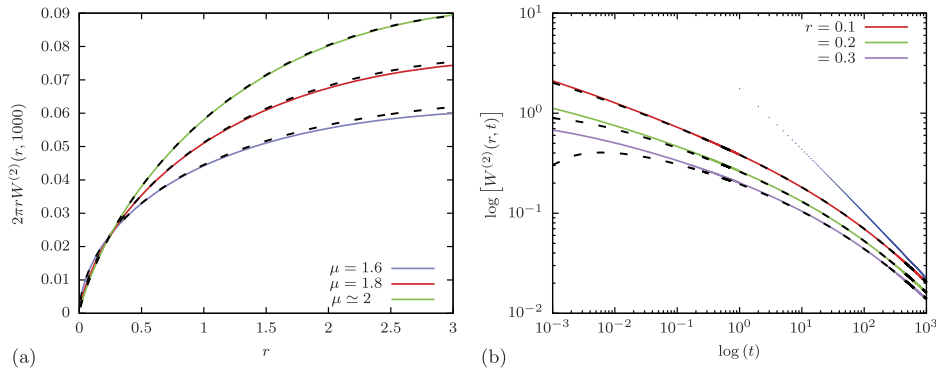
Figure 2. Two-dimensional propagator (35) (coloured solid curves) and asymptotic behaviour (37) (dashed black curves): (a) spatial evolution at time $t = 1000$ and different values of the space-fractional parameter, $\mu = 1.6$, 1.8, and $\mu \simeq 2$. (b) Temporal evolution at different distances, $r = 0.1$, 0.2, and 0.3. In panel (b), the long-time behaviour (38) (dotted blue line) is drawn at $r = 0.1$. The model parameters are chosen as $p_1 = 0.9$, $p_2 = 0.1$, $\alpha_1 = 0.3$, $\alpha_2 = 0.7$ and we show the curves of panel (b) at $\mu = 1.8$.

$$
W^{(2)}(r,t) \sim \frac{1}{4\pi(p_1 t^{\alpha_1})^{2/\mu}} \left\{ \frac{2}{\mu} \Gamma\left(1 - \frac{2}{\mu}\right) \Gamma\left(\frac{2}{\mu}\right) E^{2/\mu}_{\alpha_2-\alpha_1,\,1-2\alpha_1/\mu} \right.
$$

$$
\times \left(-\frac{p_2}{p_1} t^{\alpha_2-\alpha_1} \right) + \frac{\Gamma\left(1 - \frac{\mu}{2}\right)}{\Gamma\left(\frac{\mu}{2}\right)} \left(\frac{r^\mu}{2^\mu p_1 t^{\alpha_1}} \right)^{1-2/\mu}
$$

$$
\left. \times\, E_{\alpha_2-\alpha_1,\,1-\alpha_1}\left(-\frac{p_2}{p_1} t^{\alpha_2-\alpha_1} \right) \right\}, \quad r^\mu \ll 2^\mu p_1 t^{\alpha_1}, \tag{37}
$$

where $1 < \mu < 2$. Utilising the asymptotic behaviour of the generalised Mittag–Leffler function (A15), we obtain

$$
W^{(2)}(r,t) \sim \frac{1}{2\mu p_2^{2/\mu} \sin(2\pi/\mu)} \frac{t^{-2\alpha_2/\mu}}{\Gamma(1-2\alpha_2/\mu)}
$$

$$
+ \frac{\Gamma(1-\mu/2)r^{\mu-2}}{2^\mu \pi p_2 \Gamma(\mu/2)} \frac{t^{-\alpha_2}}{\Gamma(1-\alpha_2)}, \quad t \to \infty, \ r \to 0, \tag{38}
$$

for $1 < \mu < 2$.

Figure 2 shows a comparison of the asymptotic behaviour given in terms of the generalised Mittag–Leffler functions (37) with two and three parameters, and the two-dimensional propagator (35). We first compare them as functions of the spatial variable at different values of the space-fractional parameter μ, from which it is clear that the two-dimensional propagator (35) is well approximated by the long-time behaviour (37) near the origin, see figure 2(a). We also compare the full two-dimensional propagator (35) with the asymptote (37) as function of time in figure 2(b). When $r = 0.1$, for instance, we observe full agreement over the entire time domain shown in the plot. As r increases such that the condition $r^\mu \ll 2^\mu p_1 t^{\alpha_1}$ breaks down, the asymptotic law (37) fails to approximate the two-dimensional propagator. The long-time behaviour near the origin is represented by the dotted blue curve for the position $r = 0.1$ in figure 2(b).
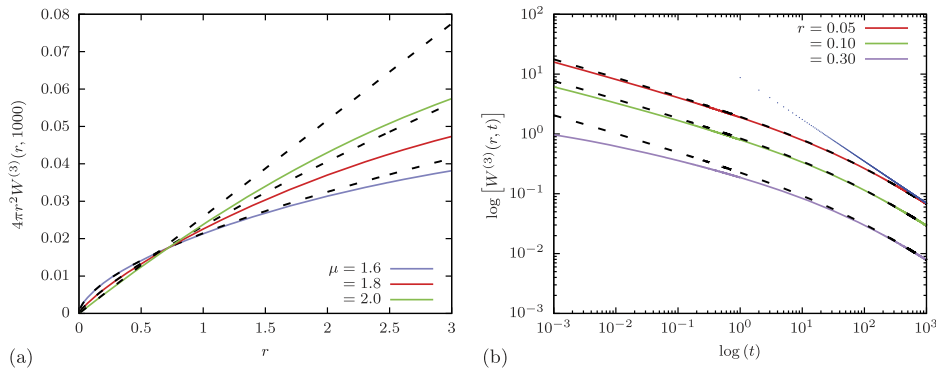
Figure 3. Asymptotic behaviour (41) (dashed black curves) along with the three-dimensional propagator (39) (coloured solid curves) (a) as functions of the space variable (multiplied by $4\pi r^2$) at time $t = 1000$ and different values of the space fractional parameter, $\mu = 1.6$, 1.8, and 2; and (b) as functions of time for different values of the radial distance r, $r = 0.05$, 0.1, and 0.3. The long-time behaviour (42) near the origin at $r = 0.05$ is shown as the dotted blue line in panel (b). The model parameters are $p_1 = 0.9$, $p_2 = 0.1$, $\alpha_1 = 0.3$, $\alpha_2 = 0.7$, and we draw the curves of panel (b) for $\mu = 1.8$.

4.1.3. 3D case. The 3D solution for the bi-fractional diffusion equation (11) reads

$$W^{(3)}(r,t) = \frac{1}{8\pi^{3/2}(p_1 t^{\alpha_1})^{3/\mu}} \sum_{k=0}^{\infty} \frac{(-1)^k}{k!} \left(\frac{p_2}{p_1} t^{\alpha_2 - \alpha_1} \right)^k$$

$$\times H_{2,3}^{2,1} \left[\frac{r^\mu}{2^\mu p_1 t^{\alpha_1}} \left| \begin{array}{c} \left(1 - k - \frac{3}{\mu}, 1\right); \left(1 - \frac{3\alpha_1}{\mu} + (\alpha_2 - \alpha_1)k, \alpha_1\right) \\ \left(0, \frac{\mu}{2}\right), \left(1 - \frac{3}{\mu}, 1\right); \left(-\frac{1}{2}, \frac{\mu}{2}\right) \end{array} \right. \right]. \quad (39)$$

With the asymptotic expression (A10) for the H-function we obtain the asymptotic form

$$W^{(3)}(r,t) \sim \frac{\Gamma(3/2 - \mu/2) r^{\mu-3}}{2^\mu \pi^{3/2} p_1 \Gamma(\mu/2) t^{\alpha_1}} \sum_{k=0}^{\infty} \frac{\left(-\frac{p_2}{p_1} t^{\alpha_2 - \alpha_1}\right)^k}{\Gamma\left(1 - \alpha_1 + (\alpha_2 - \alpha_1)k\right)}. \quad (40)$$

As before, we can rewrite this result in terms of the Mittag–Leffler function (A19) as

$$W^{(3)}(r,t) \sim \frac{\Gamma(3/2 - \mu/2) r^{\mu-3}}{2^\mu \pi^{3/2} p_1 \Gamma(\mu/2) t^{\alpha_1}} E_{\alpha_2 - \alpha_1, 1-\alpha_1} \left(-\frac{p_2}{p_1} t^{\alpha_2 - \alpha_1} \right),$$

$$r^\mu \ll 2^\mu p_1 t^{\alpha_1}, \quad (41)$$

where $1 < \mu \leqslant 2$. For very long times, from relation (A15) we obtain the leading order behaviour

$$W^{(3)}(r,t) \sim \frac{\Gamma(3/2 - \mu/2) r^{\mu-3}}{2^\mu \pi^{3/2} p_2 \Gamma(\mu/2)} \frac{t^{-\alpha_2}}{\Gamma(1 - \alpha_2)}, \quad t \to \infty, \ r \to 0, \quad (42)$$

and $1 < \mu \leqslant 2$. Again, good agreement between the asymptotic behaviours (41)–(42) and the full three-dimensional propagator (39) is observed, particularly near the origin, as

demonstrated in figure 3. It is notable that we confined the upper limit of the time scale to 10^3, and we chose $p_1 = 0.9$ and $p_2 = 0.1$. We also note that to get the asymptotic behaviours we could have used the Fourier–Laplace transform (13) and applied Tauberian theorems, thus shortening some of the calculations. However, we prefer the detailed separate derivation of the 2D and 3D cases, as this way we obtained a number of interesting closed-form results.

4.2. Behaviour at short times and/or far from the origin

We now derive explicit closed-form formulas for the short-time behaviours of the propagator (19) and/or for long distances from the origin, i.e., $r^2 \gg p_1 t^{\alpha_1}$. To this end, we use the corresponding limiting behaviour in Laplace space, $\Re\{s\} \to \infty$. Then the expressions for the propagator in n dimensions and in the limit $\mu = 2$ are given by

$$\widetilde{W}^{(1)}(x, s) = \frac{1}{2s\sqrt{p_1 s^{-\alpha_1} + p_2 s^{-\alpha_2}}} \exp\left(-\frac{|x|}{\sqrt{p_1 s^{-\alpha_1} + p_2 s^{-\alpha_2}}}\right), \tag{43}$$

$$\widetilde{W}^{(2)}(r, s) = \frac{1}{2\pi s(p_1 s^{-\alpha_1} + p_2 s^{-\alpha_2})} K_0\left(\frac{r}{\sqrt{p_1 s^{-\alpha_1} + p_2 s^{-\alpha_2}}}\right), \tag{44}$$

$$\widetilde{W}^{(3)}(r, s) = \frac{1}{4\pi r s(p_1 s^{-\alpha_1} + p_2 s^{-\alpha_2})} \exp\left(-\frac{r}{\sqrt{p_1 s^{-\alpha_1} + p_2 s^{-\alpha_2}}}\right). \tag{45}$$

For sufficiently small values of time, corresponding to sufficiently large values of the Laplace variable s, i.e., $\Re\{s\} \to \infty$ [84], we see that $p_1 s^{-\alpha_1} \gg p_2 s^{-\alpha_2}$, thus, the solutions (43)–(45) in this limit behave as

$$\widetilde{W}^{(1)}(x, s) \sim \frac{1}{2\sqrt{p_1}} s^{\alpha_1/2-1} \exp\left(-\frac{|x|}{\sqrt{p_1}} s^{\alpha_1/2}\right), \quad \Re\{s\} \to \infty, \tag{46}$$

$$\widetilde{W}^{(2)}(r, s) \sim \frac{1}{2p_1^{3/4}\sqrt{2\pi r}} s^{3\alpha_1/4-1} \exp\left(-\frac{r}{\sqrt{p_1}} s^{\alpha_1/2}\right), \quad \Re\{s\} \to \infty, \tag{47}$$

$$\widetilde{W}^{(3)}(r, s) \sim \frac{1}{4\pi p_1 r} s^{\alpha_1-1} \exp\left(-\frac{r}{\sqrt{p_1}} s^{\alpha_1/2}\right), \quad \Re\{s\} \to \infty, \tag{48}$$

where we employed the asymptotic relation $K_0(z) \sim \sqrt{\pi/2}\exp(-z)/\sqrt{z}$ as $z \to \infty$ [88]. By help of relation (A13), equations (46)–(48) can be Laplace-inverted, yielding

$$W^{(1)}(x, t) \sim \frac{1}{2\sqrt{p_1 t^{\alpha_1}}} H_{1,1}^{1,0}\left[\frac{|x|}{\sqrt{p_1 t^{\alpha_1}}} \left| \begin{matrix} \left(1 - \frac{\alpha_1}{2}, \frac{\alpha_1}{2}\right) \\ (0, 1) \end{matrix} \right.\right], \quad t \to 0, \tag{49}$$

$$W^{(2)}(r, t) \sim \frac{1}{\sqrt{8\pi r}(p_1 t^{\alpha_1})^{\frac{3}{4}}} H_{1,1}^{1,0}\left[\frac{r}{\sqrt{p_1 t^{\alpha_1}}} \left| \begin{matrix} \left(1 - \frac{3\alpha_1}{4}, \frac{\alpha_1}{2}\right) \\ (0, 1) \end{matrix} \right.\right], \quad t \to 0, \tag{50}$$

$$W^{(3)}(r, t) \sim \frac{1}{4\pi p_1 r t^{\alpha_1}} H_{1,1}^{1,0}\left[\frac{r}{\sqrt{p_1 t^{\alpha_1}}} \left| \begin{matrix} \left(1 - \alpha_1, \frac{\alpha_1}{2}\right) \\ (0, 1) \end{matrix} \right.\right], \quad t \to 0. \tag{51}$$

We note that the short-time asymptotic behaviours (49)–(51), for general $n = 1, 2, 3$, can be expressed as
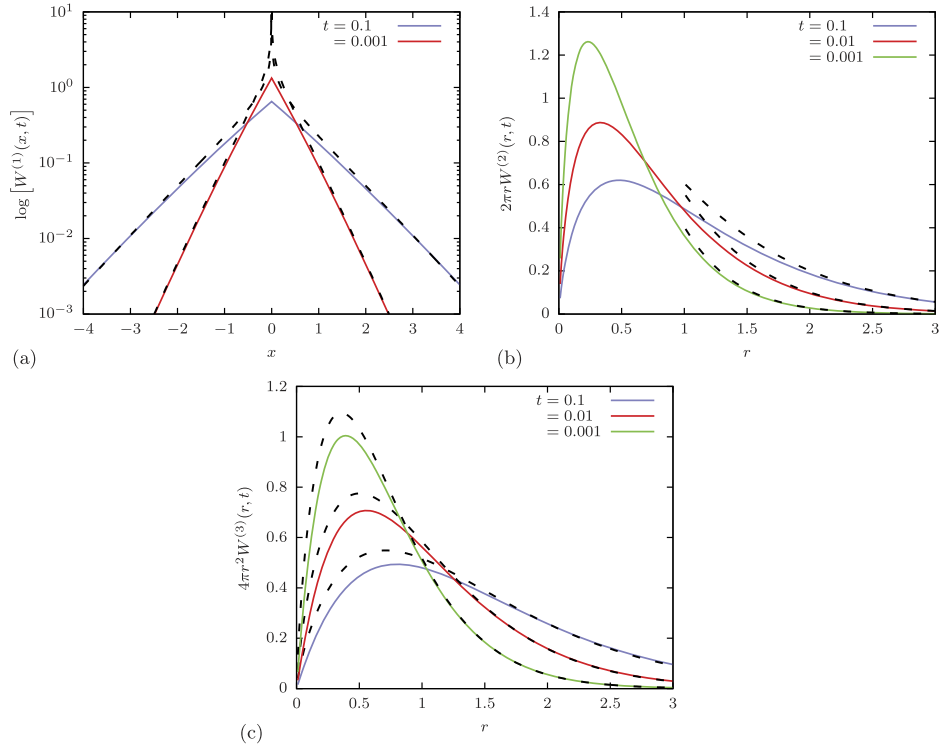
Figure 4. Spatial dependence of the n-dimensional propagator (19) (coloured solid curves) along with the stretched Gaussian shape (55) (dashed black curves). (a) Logarithm of the one-dimensional case, $n = 1$, compared with expression (55) at two time instants, $t = 0.1$ and 0.001. (b) Two-dimensional case, $n = 2$, compared with (55) at $t = 0.1$, 0.01, and 0.001. Both are multiplied by $2\pi r$. (c) Three-dimensional propagator, $n = 3$, compared with (55) at $t = 0.1$, 0.01, and 0.001. Both are multiplied by $4\pi r^2$. The model parameters are chosen as $p_1 = 0.9$, $p_2 = 0.1$, $\alpha_1 = 0.3$, and $\alpha_2 = 0.7$. In the cases $n = 1, 3$, we set $\mu = 2$, while in the case $n = 2$, $\mu \simeq 2$ ($= 1.999\,95$).

$$
W^{(n)}(r, t) \sim \frac{1}{(4p_1 t^{\alpha_1})^{\frac{n+1}{4}} (\pi r)^{\frac{n-1}{2}}} H_{1,1}^{1,0} \left[\frac{r}{\sqrt{p_1 t^{\alpha_1}}} \left| \begin{matrix} \left(1 - \frac{(n+1)\alpha_1}{4}, \frac{\alpha_1}{2}\right) \\ (0, 1) \end{matrix} \right. \right], \quad t \to 0. \tag{52}
$$

Finally, we derive a stretched Gaussian behaviour for equation (52). Using equations (A11) and (A12) we find the asymptotic behaviour

$$
H_{1,1}^{1,0} \left[\frac{r}{\sqrt{p_1 t^{\alpha_1}}} \left| \begin{matrix} \left(1 - \frac{(n+1)\alpha_1}{4}, \frac{\alpha_1}{2}\right) \\ (0, 1) \end{matrix} \right. \right] \sim \frac{1}{\sqrt{\pi(2 - \alpha_1)}} \left(\frac{\alpha_1 r}{2\sqrt{p_1 t^{\alpha_1}}} \right)^{\frac{(n+1)\alpha_1 - 2}{2(2 - \alpha_1)}}
$$

$$
\times \operatorname{Exp}_f \left(\frac{r}{\sqrt{p_1 t^{\alpha_1}}} \right), \tag{53}
$$

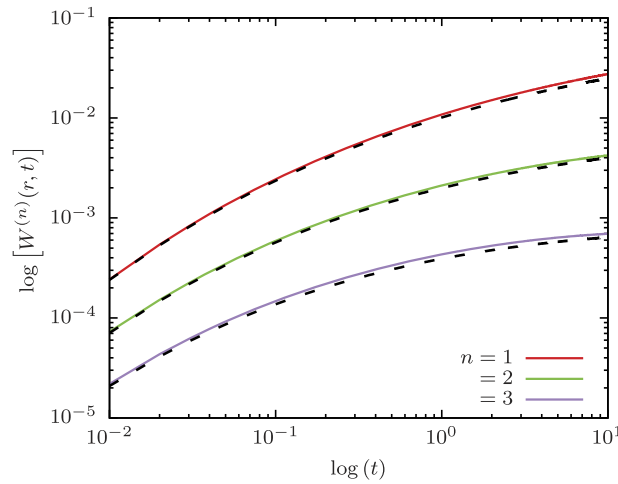valid for $r^2 \gg p_1 t^{\alpha_1}$, where we abbreviate

Figure 5. A comparison between the stretched Gaussian behaviour (55) (dashed black curves) and the full n-dimensional propagator (19) (coloured solid curves) as function of time at fixed position $r = 4$, on the log–log scale. For the one-dimensional case, $n = 1$, and the three-dimensional case, $n = 3$, we set $\mu = 2$ in (19), while for the two-dimensional case, $n = 2$, we set $\mu = 1.99995$, i.e., $\mu \simeq 2$. The other model parameters are chosen as $p_1 = 0.9$, $p_2 = 0.1$, $\alpha_1 = 0.3$, and $\alpha_2 = 0.7$.

$$
\mathrm{Exp}_f\left(\frac{r}{\sqrt{p_1 t^{\alpha_1}}}\right) = \exp\left(-\left(1 - \frac{\alpha_1}{2}\right)\left(\frac{\alpha_1}{2}\right)^{\alpha_1/(2-\alpha_1)}\left(\frac{r}{\sqrt{p_1 t^{\alpha_1}}}\right)^{2/(2-\alpha_1)}\right).
$$
(54)

In view of relations (53) and (54), we arrive at the short-time behaviour (and/or far from the origin)

$$
W^{(n)}(r,t) \sim \frac{\pi^{-n/2}}{\sqrt{2 - \alpha_1}} \alpha_1^{\frac{(n+1)\alpha_1 - 2}{2(2-\alpha_1)}} (4 p_1 t^{\alpha_1})^{-\frac{n}{2(2-\alpha_1)}} r^{-\frac{n(1-\alpha_1)}{2-\alpha_1}} \mathrm{Exp}_f\left(\frac{r}{\sqrt{p_1 t^{\alpha_1}}}\right),
$$
(55)

where $r^2 \gg p_1 t^{\alpha_1}$.

In figure 4 we present the spatial evolution of both the full n-dimensional propagator (19) and the stretched Gaussian behaviour (55) for different n. The propagator (19) can be accurately described by the stretched Gaussian shape in the short-time regime and/or far from the origin. Furthermore, figure 5 compares the asymptotic behaviour (55) with the n-dimensional propagator (19) at the fixed position $r = 4$, showing the agreement with the stretched Gaussian behaviour.

5. Statistical properties

We now proceed to derive the moments and explore in detail the MSD, skewness and kurtosis of the PDF $W^{(n)}(\mathbf{r}, t)$ in n dimensions. First, we note that the PDF is normalised. The 0th moment can be calculated by help of equation (13) as

$$\int_{\mathbb{R}^n} W^{(n)}(\mathbf{r},t)\mathrm{d}^n\mathbf{r} = \mathscr{F}_n\left\{W^{(n)}(\mathbf{r},t)\right\}(\mathbf{q}=0,t) = 1, \tag{56}$$

where $\mathscr{F}_n\left\{f^{(n)}(\mathbf{r},t)\right\}(\mathbf{q},t) = \int_{\mathbb{R}^n} f^{(n)}(\mathbf{r},t)\exp(\imath\mathbf{q}\cdot\mathbf{r})\mathrm{d}^n\mathbf{r}$. Therefore, the nonzero even moments are given through the function [57, 89]

$$M(2m_1,\ldots,2m_n) = \int_{\mathbb{R}^n} x_1^{2m_1}\ldots x_n^{2m_n} W^{(n)}(\mathbf{r},t)\mathrm{d}^n\mathbf{r} \tag{57}$$

$$= \int_{\mathbb{R}^n} e_1^{2m_1}\ldots e_n^{2m_n} W^{(n)}(\mathbf{r},t)r^{2m}\mathrm{d}^n\mathbf{r} \tag{58}$$

$$= \int_{\mathbb{R}^n} e_1^{2m_1}\ldots e_n^{2m_n} W^{(n)}(\mathbf{r},t)r^{2m}r^{n-1}\,\mathrm{d}r\,\mathrm{d}^{n-1}\mathbf{e}, \tag{59}$$

where m_i is a positive integer for all $i=1,2,\ldots,n$, $m=\sum_{i=1}^n m_i$, $\mathrm{d}^{n-1}\mathbf{e}$ is the angular integral element, $\mathbf{e}=(e_1,\ldots,e_n)$ is the radial unit vector, and $e_i=x_i/r$, $i=1,2\ldots,n$. Then, we can express the moments in terms of the Mellin transform of the propagator [21],

$$M(2m_1,\ldots,2m_n) = \left(\int_{\mathbb{R}^{n-1}} e_1^{2m_1}\ldots e_n^{2m_n}\mathrm{d}^{n-1}\mathbf{e}\right)$$

$$\times\left(\int_0^\infty r^{2m+n-1}W^{(n)}(r,t)\mathrm{d}r\right)$$

$$= \Omega_n(m_1,\ldots,m_n,n)\left(\mathscr{M}W^{(n)}(r,t)\right)(2m+n,t), \tag{60}$$

where

$$\Omega_n(m_1,\ldots,m_n,n) = \int_{\mathbb{R}^{n-1}} e_1^{2m_1}\ldots e_n^{2m_n}\mathrm{d}^{n-1}\mathbf{e}$$

$$= \frac{2}{\Gamma(m+n/2)}\prod_{i=1}^n \Gamma\left(m_i+\frac{1}{2}\right), \tag{61}$$

and the Mellin transform for any generic function is defined as $\mathscr{M}\{f(x)\}(z) = \breve{f}(z) = \int_0^\infty x^{z-1}f(x)\mathrm{d}x$. Returning to the propagator (19) with $\mu=2$, the Mellin transform of $W^{(n)}(r,t)$ with respect to r is given as

$$\left(\mathscr{M}W^{(n)}(r,t)\right)(z,t) = \frac{1}{2\pi^{\frac{n}{2}}}\left(\frac{1}{4p_1t^{\alpha_1}}\right)^{\frac{n-z}{2}}\sum_{k=0}^\infty \frac{(-1)^k}{k!}\left(\frac{p_2}{p_1}t^{\alpha_2-\alpha_1}\right)^k$$

$$\times\frac{\Gamma\left(\frac{z}{2}\right)\Gamma\left(1-\frac{n}{2}+\frac{z}{2}\right)\Gamma\left(k+\frac{n}{2}-\frac{z}{2}\right)}{\Gamma\left(\frac{n}{2}-\frac{z}{2}\right)\Gamma\left(1-\frac{n\alpha_1}{\mu}+(\alpha_2-\alpha_1)k+\frac{\alpha_1 z}{2}\right)}. \tag{62}$$

Thus,

$$\left(\mathscr{M}W^{(n)}(r,t)\right)(2m+n,t) = \frac{1}{2\pi^{\frac{n}{2}}}\Gamma\left(m+\frac{n}{2}\right)\Gamma(1+m)(4p_1t^{\alpha_1})^m$$

$$\times\sum_{k=0}^\infty \frac{(-m)_k}{\Gamma(1+m\alpha_1+(\alpha_2-\alpha_1)k)}\frac{\left(-\frac{p_2}{p_1}t^{\alpha_2-\alpha_1}\right)^k}{k!}, \tag{63}$$

where $(-m)_k = \Gamma(k - m)/\Gamma(-m)$. Again, from definition (A14) of the generalised Mittag–Leffler function, the Mellin transform (63) can be written in the form

$$\left(\mathcal{M}W^{(n)}(r, t)\right)(2m + n, t) = 2^{2m-1}\pi^{-\frac{n}{2}}\Gamma\left(m + \frac{n}{2}\right)\Gamma(1 + m)\, p_1^m t^{\alpha_1 m}$$

$$\times E_{\alpha_2 - \alpha_1, m\alpha_1 + 1}^{-m}\left(-\frac{p_2}{p_1}t^{\alpha_2 - \alpha_1}\right). \tag{64}$$

By help of this expression we re-express the moment function (60) as

$$M(2m_1, \ldots, 2m_n) = C_{m,n}\, p_1^m t^{\alpha_1 m} E_{\alpha_2 - \alpha_1, m\alpha_1 + 1}^{-m}\left(-\frac{p_2}{p_1}t^{\alpha_2 - \alpha_1}\right), \tag{65}$$

where

$$C_{m,n} = 2^{2m}\pi^{-n/2}\Gamma(1 + m)\prod_{i=1}^{n}\Gamma\left(m_i + \frac{1}{2}\right). \tag{66}$$

The short-time and long-time behaviours of the moment function (65) can then be deduced from the asymptotic behaviour (A15) of the generalised Mittag–Leffler function (A15),

$$M(2m_1, \ldots, 2m_n) \sim C_{mn}\begin{cases}\dfrac{(p_1 t^{\alpha_1})^m}{\Gamma(1 + m\alpha_1)}, & t \to 0^+ \\[2ex] \dfrac{(p_2 t^{\alpha_2})^m}{\Gamma(1 + m\alpha_2)}, & t \to \infty\end{cases}, \tag{67}$$

namely, an accelerating crossover behaviour, as it should be. If $m = 1$, the moment function $M(\cdot)$ provides an accelerating subdiffusive crossover.

We note that while the radial functions $W^{(2)}(r, t)$ and $W^{(3)}(r, t)$ diverge near $r = 0$, the proper expressions including the volume elements $2\pi r$ and $4\pi r^2$ guarantee normalisation, see also [73, 90]. Note that the non-negativity was demonstrated in section 3.

We first evaluate the qth order moments. The MSD, the skewness and the kurtosis of any PDF, significant statistical properties of a random variable, are respectively defined for a generic random variable X as

$$\mathrm{MSD}_X(t) = \langle X^2 \rangle - \langle X \rangle^2, \tag{68a}$$

$$\mathrm{Skew}_X(t) = \frac{\left\langle \left(X - \langle X \rangle\right)^3 \right\rangle}{\left\langle \left(X - \langle X \rangle\right)^2 \right\rangle^{3/2}}, \tag{68b}$$

$$\mathrm{Kurt}_X(t) = \frac{\left\langle \left(X - \langle X \rangle\right)^4 \right\rangle}{\left\langle \left(X - \langle X \rangle\right)^2 \right\rangle^2}. \tag{68c}$$

In the one-dimensional force-free case, we have that $\langle x \rangle = \langle x^3 \rangle = \cdots = 0$, thus the MSD is itself the second moment (B3), i.e.,

$$\mathrm{MSD}_1(t) = 2\left[\frac{p_1 t^{\alpha_1}}{\Gamma(1 + \alpha_1)} + \frac{p_2 t^{\alpha_2}}{\Gamma(1 + \alpha_2)}\right], \tag{69}$$

with the asymptotic behaviours

$$\text{MSD}_1(t) \simeq \begin{cases} \dfrac{2p_1 t^{\alpha_1}}{\Gamma(1+\alpha_1)}, & t \to 0^+ \\ \dfrac{2p_2 t^{\alpha_2}}{\Gamma(1+\alpha_2)}, & t \to \infty \end{cases}, \tag{70}$$

namely, the accelerating subdiffusion crossover built into our model. Moreover, the skewness of the one-dimensional PDF is zero and the curve is totally symmetric about its mean value $\langle x \rangle = 0$. Finally the kurtosis in the one-dimensional case is given by

$$\text{Kurt}_1(t) = \frac{\langle x^4 \rangle}{\langle x^2 \rangle^2} = \frac{6 \left[\frac{p_1^2 t^{2\alpha_1}}{\Gamma(1+2\alpha_1)} + \frac{2p_1 p_2 t^{\alpha_1+\alpha_2}}{\Gamma(1+\alpha_1+\alpha_2)} + \frac{p_2^2 t^{2\alpha_2}}{\Gamma(1+2\alpha_2)} \right]}{\left[\frac{p_1 t^{\alpha_1}}{\Gamma(1+\alpha_1)} + \frac{p_2 t^{\alpha_2}}{\Gamma(1+\alpha_2)} \right]^2}. \tag{71}$$

In the case $\alpha_1 = \alpha_2 = 1$, (11) with $\mu = 2$ reduces to the normal diffusion equation and (71) reduces to the expected result $\text{Kurt}_1 = 3$, the kurtosis of the normal 'Gaussian' distribution in one-dimension.

In view of the higher-dimension cases, we understand that the first moment of these distributions is non-zero, thus, there should be a non-zero skewness, refer to figure 4. The MSD, the skewness and the kurtosis in higher dimensions are given by

$$\text{MSD}(t) = \langle r^2 \rangle - r_0^2, \tag{72a}$$

$$\text{Skew}(t) = \frac{\langle r^3 \rangle - 3r_0 \langle r^2 \rangle + 2r_0^3}{\left[\langle r^2 \rangle - r_0^2 \right]^{3/2}}, \tag{72b}$$

$$\text{Kurt}(t) = \frac{\langle r^4 \rangle - 4r_0 \langle r^3 \rangle + 6r_0^2 \langle r^2 \rangle - 3r_0^4}{\langle r^2 \rangle^2 - 2r_0^2 \langle r^2 \rangle + r_0^4}, \tag{72c}$$

where $r_0 = \langle r \rangle$. The MSD of the two-dimensional PDF $W^{(2)}(\mathbf{q}, t)$ has the asymptotic behaviours, see equations (B8) and (B11),

$$\text{MSD}_2(t) \simeq \begin{cases} 4p_1 t^{\alpha_1} \left[\dfrac{1}{\Gamma(1+\alpha_1)} - \dfrac{\left[\Gamma\left(\frac{3}{2}\right) \right]^4}{\left[\Gamma\left(1+\frac{\alpha_1}{2}\right) \right]^2} \right], & t \to 0^+, \\ 4p_2 t^{\alpha_2} \left[\dfrac{1}{\Gamma(1+\alpha_2)} - \dfrac{\left[\Gamma\left(\frac{3}{2}\right) \right]^4}{\left[\Gamma\left(1+\frac{\alpha_2}{2}\right) \right]^2} \right], & t \to \infty, \end{cases} \tag{73}$$

where $0 < 1/\Gamma(1+\alpha) - \left[\Gamma\left(\frac{3}{2}\right) \right]^4 / \left[\Gamma\left(1+\frac{\alpha}{2}\right) \right]^2 < 0.41$ for $0 < \alpha < 1$. Analogously, the MSD of the three-dimensional PDF $W^{(3)}(\mathbf{q}, t)$ has the asymptotic behaviours, see equations (B13) and (B16),

$$\text{MSD}_3(t) \simeq \begin{cases} 2p_1 t^{\alpha_1} \left[\dfrac{3}{\Gamma(1+\alpha_1)} - \dfrac{2}{\left[\Gamma\left(1+\frac{\alpha_1}{2}\right) \right]^2} \right], & t \to 0^+, \\ 2p_2 t^{\alpha_2} \left[\dfrac{3}{\Gamma(1+\alpha_2)} - \dfrac{2}{\left[\Gamma\left(1+\frac{\alpha_2}{2}\right) \right]^2} \right], & t \to \infty, \end{cases} \tag{74}$$

where $0 < 3/\Gamma(1+\alpha) - 2/\left[\Gamma\left(1+\frac{\alpha}{2}\right) \right]^2 < 1.058$ for $0 < \alpha < 1$. It is obvious from the asymptotic behaviours (73) and (74) that the PDFs $W^{(2)}(\mathbf{q}, t)$ and $W^{(3)}(\mathbf{q}, t)$ preserve an accelerating subdiffusion crossover like its counterpart in the one-dimensional case, see equation (70).
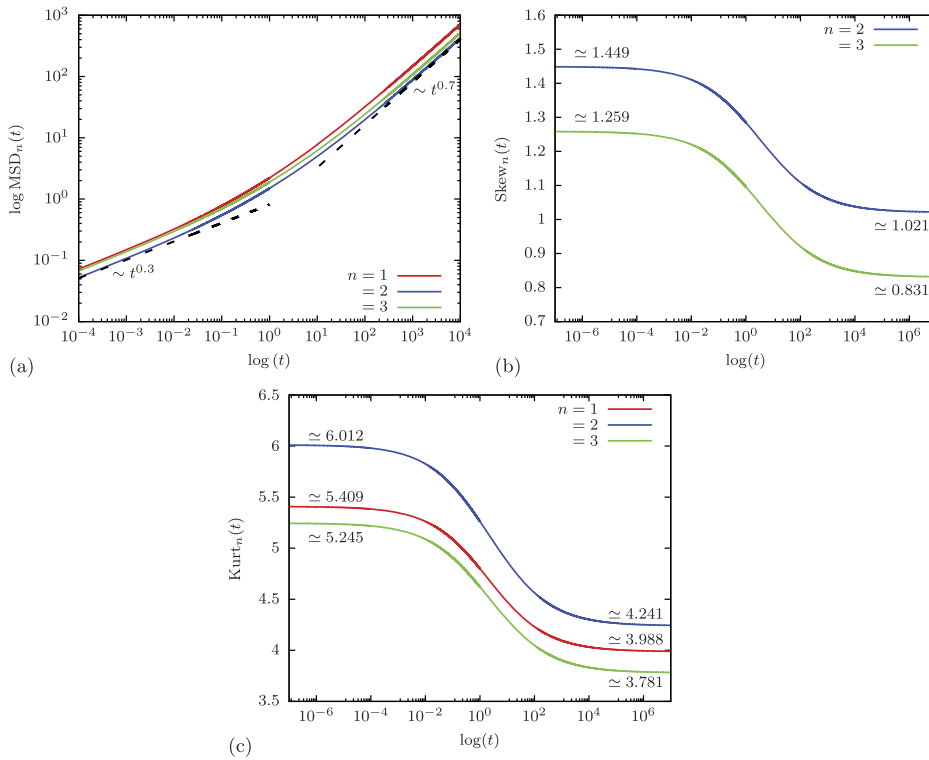
Figure 6. Statistical properties of the PDFs $W^{(n)}(\mathbf{q}, t)$, $n = 1, 2, 3$; (a) MSD (69) and (72a) on the log–log scale with their asymptotic behaviours (70), (73) and (74); (b) skewness (72b) for the two- and three-dimensional PDFs with their asymptotic values and (c) kurtosis for the one-dimension (71) and two- and three-dimension (72c) with their asymptotic values, all are computed for the fractional parameters $\alpha_1 = 0.3$ and $\alpha_2 = 0.7$. The other model parameters are $p_1 = 0.5$, $p_2 = 0.5$, and $\mu = 2$ for all panels.

In figure 6 we show the exact forms for the MSD, the skewness, and the kurtosis. To see the exact crossover behaviours for the MSD, we use log–log scales while single-log scales are used for the skewness and kurtosis. The asymptotes according to equations (70), (73), and (74) are also shown for the MSD. It is found that both skewness and kurtosis in general have different asymptotic values in the short- and long-time regimes. This can be easily demonstrated by direct substitution from the asymptotic behaviours of the qth order moments in appendix B into the exact forms (72). Since the skewness of the one-dimensional case is zero, we do not show it in figure 6(b). As figures 4(b) and (c) showed right-skewed curves, the skewness of the two- and three-dimensional PDFs are positive. The kurtosis exceeds 3 ($\text{Kurt}_n > 3$) in the one-, two-, and three-dimensional cases.

6. Conclusions

We investigated the propagator governed by the bi-factional diffusion equation of the modified type, with and without space-fractality, in the n-dimensional case, describing accelerating diffusion crossover. This complements our recent study of the corresponding natural type equation exhibiting a retarding diffusive crossover [67]. We derived the multidimensional propagator

as an infinite series of the Fox H-function, which also generalises its counterpart in the one-dimensional setting [79]. The method of solution was employed in [82] for an averaged generalised fractional elastic model, and developed in [67] for the multidimensional bi-fractional diffusion equation of the natural type as a generalisation of the Schneider–Wyss solution [57] and the subordination approach. The space fractality was included here in analogy to [67], to avoid divergence of the series expansion of the H-function in (19) when $n = 2$ and $\mu = 2$. The two-dimensional solution of the bi-fractional diffusion equation without space fractality was obtained through the limit $\mu \to 2$. We proved the non-negativity of the propagator (19) in higher dimensions, an indispensable property to guarantee the probabilistic interpretation of the process, by invoking two different techniques. Moreover, we derived the asymptotic behaviours for the propagator (19) in terms of generalised Mittag–Leffler functions when $r^\mu \ll 2^\mu p_1 t^{\alpha_1}$, and in terms of a simpler form of the H-function when $t \to 0$. In particular, we provided a stretched Gaussian shape for the short-time regime $r^2 \gg p_1 t^{\alpha_1}$, similar to the results in [21, 57, 73].

The relevance of the bi-fractional diffusion equation of the modified type stems from the accelerating crossover behaviour displayed by the associated MSD. We showed that this accelerating subdiffusion known from the one-dimensional formulation in [65] is also preserved in the higher dimensions, and we quantified the dynamic behaviours in terms of the MSD, the skewness and the kurtosis.

The approach based on the bi-fractional diffusion equations of natural and modified types can be derived from the CTRW picture in the one-dimensional case [86]. In this formulation the crossover behaviour is included through the specific choice of the waiting time PDF [86]. An explicit derivation for our higher-dimensional case is part of our ongoing work. We note that there exist alternative descriptions of crossover dynamics. In particular we mention exponential and power-law tempering of long-range correlations in the driving noise in fractional Brownian motion and the fractional Langevin equation [96]. Alternative tempering of fractional Brownian motion instead lead to confinement effects [96, 97]. In a CTRW formulation a crossover from subdiffusion to normal diffusion is realised in subdiffusive CTRWs to which diffusive noise is superimposed [98], similar to tempering a scale-free waiting time PDF [99]. We finally note the discussion of crossovers in a CTRW model with Prabhakar generalised Mittag–Leffler waiting times [100, 101].

Acknowledgments

Data availability statement

No new data were created or analysed in this study.

Appendix A. Special functions

We here summarise some special functions which are used throughout the paper. The Fox H-function is defined in terms of the Mellin–Barnes integral [91]

$$H_{p,q}^{m,n}\left[x \left| \begin{array}{l} (a_1, A_1), \ldots, (a_p, A_p) \\ (b_1, B_1), \ldots, (b_q, B_q) \end{array} \right. \right] = \frac{1}{2\pi i} \int_\Omega \Theta(s) \, x^s \, ds, \tag{A1}$$

where m, n, p, and q are integers satisfying $0 \leqslant n \leqslant p$, $1 \leqslant m \leqslant q$, $a_i, b_j \in \mathbb{C}$, $A_i, B_j \in \mathbb{R}_+$, $i = 1, \ldots, p$, $j = 1, \ldots, q$, and the function $\Theta(s)$ is given by

$$\Theta(s) = \frac{\prod_{j=1}^{m} \Gamma(b_j - B_j s) \prod_{j=1}^{n} \Gamma(1 - a_j + A_j s)}{\prod_{j=m+1}^{q} \Gamma(1 - b_j + B_j s) \prod_{j=n+1}^{p} \Gamma(a_j - A_j s)}, \tag{A2}$$

where $\Gamma(\cdot)$ is the gamma function. The contour Ω on the right-hand side of equation (A1) separates the poles of $\Gamma(b_j + B_j s)$, $j = 1, \ldots, m$ from the poles of $\Gamma(1 - a_i - A_i s)$, $i = 1, \ldots, n$. If the poles of $\prod_{j=1}^{m} \Gamma(b_j - B_j s)$ are simple, the following series expansion holds true

$$H_{p,q}^{m,n}\left[x \, \middle| \, \begin{matrix} (a_p, A_p) \\ (b_q, B_q) \end{matrix}\right]$$

$$= \sum_{h=1}^{m} \sum_{\nu=0}^{\infty} \frac{(-1)^\nu x^{\frac{b_h + \nu}{B_h}}}{\nu! B_h}$$

$$\times \frac{\prod_{j=1, j \neq h}^{m} \Gamma\left(b_j - B_j \frac{b_h + \nu}{B_h}\right) \prod_{j=1}^{n} \Gamma\left(1 - a_j + A_j \frac{b_h + \nu}{B_h}\right)}{\prod_{j=m+1}^{q} \Gamma\left(1 - b_j + B_j \frac{b_h + \nu}{B_h}\right) \prod_{j=n+1}^{p} \Gamma\left(a_j - A_j \frac{b_h + \nu}{B_h}\right)}. \tag{A3}$$

The Mellin transform of the H-function is defined by

$$\int_0^\infty x^{z-1} H_{p,q}^{m,n}\left[ax \, \middle| \, \begin{matrix} (a_p, A_p) \\ (b_q, B_q) \end{matrix}\right] \mathrm{d}x = a^{-z} \Theta(-z), \tag{A4}$$

where $\Theta(z)$ is given by (A2).

Using expansion (A3) one can obtain the special case

$$H_{2,3}^{2,1}\left[z \, \middle| \, \begin{matrix} \left(1 - k - \dfrac{n}{\mu}, 1\right) ; (a, b) \\ \left(0, \dfrac{\mu}{2}\right), \left(1 - \dfrac{n}{\mu}, 1\right) ; \left(1 - \dfrac{n}{2}, \dfrac{\mu}{2}\right) \end{matrix}\right]$$

$$= \frac{2}{\mu} \sum_{\nu=0}^{\infty} \left[\frac{(-1)^\nu}{\nu!} z^{\frac{2\nu}{\mu}} \frac{\Gamma\left(1 - \frac{n}{\mu} - \frac{2\nu}{\mu}\right) \Gamma\left(k + \frac{n}{\mu} + \frac{2\nu}{\mu}\right)}{\Gamma\left(\frac{n}{2} + \nu\right) \Gamma\left(a - \frac{2b\nu}{\mu}\right)} \right]$$

$$+ \sum_{\nu=0}^{\infty} \left[\frac{(-1)^\nu}{\nu!} z^{1 - \frac{n}{\mu} + \nu} \frac{\Gamma\left(\frac{n}{2} - \frac{\mu}{2}(1 + \nu)\right) \Gamma(1 + k + \nu)}{\Gamma\left(\frac{\mu}{2}(1 + \nu)\right) \Gamma\left(a - b\left(1 - \frac{n}{\mu} + \nu\right)\right)} \right]. \tag{A5}$$

The asymptotic behaviour of the H-function near zero is given to leading order by [91, 92]

$$H_{p,q}^{m,n}\left[z \, \middle| \, \begin{matrix} (a_p, A_p) \\ (b_q, B_q) \end{matrix}\right] \simeq |z|^c, \quad |z| \to 0, \tag{A6}$$

where $c = \min_{1 \leqslant j \leqslant m}\{\mathfrak{R}(b_j)/B_j\}$, and provided that $\rho > 0$, $|\arg z| < \frac{1}{2}\pi\rho$, and ρ is given by

$$\rho = \sum_{j=1}^{n} A_j - \sum_{j=n+1}^{p} A_j + \sum_{j=1}^{m} B_j - \sum_{j=m+1}^{q} B_j. \tag{A7}$$

Using the asymptotic behaviour (A6) and the series expansion (A3) of the H-function, we obtain

$$H_{2,3}^{2,1}\left[z\left|\begin{array}{l}\left(1-k-\dfrac{1}{\mu},1\right);(a,b)\\\left(0,\dfrac{\mu}{2}\right),\left(1-\dfrac{1}{\mu},1\right);\left(\dfrac{1}{2},\dfrac{\mu}{2}\right)\end{array}\right.\right]\sim\dfrac{2}{\mu}\dfrac{\Gamma\left(1-\frac{1}{\mu}\right)\Gamma\left(k+\frac{1}{\mu}\right)}{\Gamma\left(\frac{1}{2}\right)\Gamma(a)},\quad|z|\to0,$$

(A8)

$$H_{2,3}^{2,1}\left[z\left|\begin{array}{l}\left(1-k-\dfrac{2}{\mu},1\right);(a,b)\\\left(0,\dfrac{\mu}{2}\right),\left(1-\dfrac{2}{\mu},1\right);\left(0,\dfrac{\mu}{2}\right)\end{array}\right.\right]$$

$$\sim\dfrac{2}{\mu}\dfrac{\Gamma\left(1-\frac{2}{\mu}\right)\Gamma\left(k+\frac{2}{\mu}\right)}{\Gamma(a)}+\dfrac{\Gamma\left(1-\frac{\mu}{2}\right)\Gamma(1+k)}{\Gamma\left(\frac{\mu}{2}\right)\Gamma\left(a-b\left(1-\frac{2}{\mu}\right)\right)}z^{1-\frac{2}{\mu}},\quad|z|\to0,$$

(A9)

$$H_{2,3}^{2,1}\left[z\left|\begin{array}{l}\left(1-k-\dfrac{3}{\mu},1\right);(a,b)\\\left(0,\dfrac{\mu}{2}\right),\left(1-\dfrac{3}{\mu},1\right);\left(-\dfrac{1}{2},\dfrac{\mu}{2}\right)\end{array}\right.\right]\sim\dfrac{\Gamma\left(\frac{3}{2}-\frac{\mu}{2}\right)\Gamma(1+k)}{\Gamma\left(\frac{\mu}{2}\right)\Gamma\left(a-b\left(1-\frac{3}{\mu}\right)\right)}z^{1-\frac{3}{\mu}},\quad|z|\to0.$$

(A10)

The asymptotic behaviour of the H-function with $n=0$ for large values reads [92]

$$H_{p,q}^{m,0}\left[z\left|\begin{array}{l}(a_p,A_p)\\(b_q,B_q)\end{array}\right.\right]\sim\kappa z^{\gamma/\delta}\exp\left[-\delta(\varepsilon z)^{1/\delta}\right],\quad|z|\to\infty,$$ (A11)

where

$$\delta=\sum_{j=1}^{q}B_j-\sum_{j=1}^{p}A_j,\gamma=\sum_{j=1}^{q}b_j-\sum_{j=1}^{p}a_j+\dfrac{p-q+1}{2},\varepsilon=\prod_{j=1}^{p}A_j^{A_j}\prod_{j=1}^{q}B_j^{-B_j},$$

$$\kappa=(2\pi)^{\frac{q-p-1}{2}}\varepsilon^{\gamma/\delta}\delta^{-1/2}\prod_{j=1}^{p}A_j^{\frac{1}{2}-a_j}\prod_{j=1}^{q}B_j^{b_j-\frac{1}{2}}.$$

(A12)

The following inverse Laplace transform relation is used throughout the paper

$$\mathscr{L}^{-1}\left\{s^{-\rho}\exp\left(-as^{\sigma}\right)\right\}=t^{\rho-1}H_{1,1}^{1,0}\left[\dfrac{a}{t^{\sigma}}\left|\begin{array}{l}(\rho,\sigma)\\(0,1)\end{array}\right.\right],\quad a,\sigma>0.$$ (A13)

The Prabhakar generalisation of Mittag–Leffler function (PML) in series form reads [93–95]

$$E_{\alpha,\beta}^{\gamma}(z)=\sum_{n=0}^{\infty}\dfrac{(\gamma)_n}{\Gamma(\alpha n+\beta)}\dfrac{z^n}{n!},\quad\alpha,\beta,\gamma,z\in\mathbb{C},\ \Re\{\alpha\}>0,$$ (A14)

where $(\gamma)_n$ is the ascending Pochhammer symbol defined by $(\gamma)_0 = 1$, $(\gamma)_n = \gamma(\gamma + 1)\ldots(\gamma + n - 1) = \Gamma(\gamma + n)/\Gamma(\gamma)$. The PML function $E_{\alpha,\beta}^{\gamma}(-\lambda t^{\alpha})$ is a CMF for $t \geqslant 0$, where λ is positive constant, $0 < \alpha, \beta \leqslant 1$, and $0 < \gamma \leqslant \beta/\alpha$, and it has the asymptotic representation

$$
E_{\alpha,\beta}^{\gamma}(-\lambda t^{\alpha}) \sim
\begin{cases}
\dfrac{1}{\Gamma(\beta)} - \dfrac{\lambda\gamma t^{\alpha}}{\Gamma(\alpha + \beta)}, & t \to 0^+; \\[2ex]
\dfrac{(\lambda t^{\alpha})^{-\gamma}}{\Gamma(\beta - \alpha\gamma)}, & t \to \infty,
\end{cases}
\tag{A15}
$$

where the short-time behaviour is deduced from the series representation (A14) and the long-time behaviour can be obtained from the series

$$
E_{\alpha,\beta}^{\gamma}(-z) = \frac{z^{-\gamma}}{\Gamma(\gamma)} \sum_{n=0}^{\infty} \frac{\Gamma(n + \gamma)}{\Gamma[\beta - \alpha(n + \gamma)]} \frac{(-z)^{-n}}{n!}, \quad |z| \to \infty.
\tag{A16}
$$

The Laplace transform of the PML function is given by

$$
\mathscr{L}\left\{t^{\beta-1} E_{\alpha,\beta}^{\gamma}(-\lambda t^{\alpha}); s\right\} = \frac{s^{\alpha\gamma - \beta}}{(s^{\alpha} + \lambda)^{\gamma}}.
\tag{A17}
$$

The Hankel transform of the PML function is given by

$$
\int_0^{\infty} x^{\rho-1} J_{\nu}(ax) E_{\alpha,\beta}^{\gamma}(-bx^{\sigma}) \, \mathrm{d}x = \frac{2^{\rho-1}}{a^{\rho}\Gamma(\gamma)}
$$

$$
\times H_{2,3}^{2,1}\left[\frac{1}{b}\left(\frac{a}{2}\right)^{\sigma} \middle| \begin{array}{c} (1,1) \; ;(\beta,\alpha) \\ \left(\dfrac{\rho + \nu}{2}, \dfrac{\sigma}{2}\right), (\gamma, 1); \left(\dfrac{\rho - \nu}{2}, \dfrac{\sigma}{2}\right) \end{array}\right],
\tag{A18}
$$

which can be readily derived from the relation between the generalised Mittag–Leffler function and the Fox H-function, and the Hankel transform of the Fox H-function [91].

When $\gamma = 1$ in (A14), the PML function reduces to the generalised Mittag–Leffler function with two parameters

$$
E_{\alpha,\beta}^{1}(z) = E_{\alpha,\beta}(z) = \sum_{n=0}^{\infty} \frac{z^n}{\Gamma(\alpha n + \beta)}, \quad \alpha, \beta, z \in \mathbb{C}, \; \mathfrak{R}\{\alpha\} > 0.
\tag{A19}
$$

Similar relations for the generalised Mittag–Leffler function (A19) can be deduced by setting $\gamma = 1$ in equations (A15)–(A18). Lastly, when $\beta = 1$ in (A19), we recover the classical Mittag–Leffler function $E_{\alpha,1}(z) = E_{\alpha}(z)$.

Appendix B. qth order moments

Here we provide the qth order moments for the three PDFs in the one-dimensional, two-dimensional and three-dimensional cases, respectively.

B1. 1D PDF

The qth order moments of the PDF $W^{(1)}(x, t)$, in the one-dimensional setting, are determined through

$$\langle |x|^q \rangle (t) = \int_{-\infty}^{\infty} |x|^q W^{(1)}(|x|, t) \mathrm{d}x, \tag{B1}$$

thereby all odd moments vanish in this case, namely, $\langle x \rangle = \langle x^3 \rangle = \cdots = 0$. The qth order moment is given in Laplace space as

$$\langle x^q \rangle (s) = \frac{1}{s \sqrt{p_1 s^{-\alpha_1} + p_2 s^{-\alpha_2}}} \mathcal{M} \left\{ \exp \left(-\frac{x}{\sqrt{p_1 s^{-\alpha_1} + p_2 s^{-\alpha_2}}} \right) \right\} (q+1), \tag{B2}$$

where $\mathcal{M}\{\cdot\}$ is the Mellin transform defined for any generic function $f(x), x \geqslant 0$, by the integral $\mathcal{M}\{f(x)\}(z) = \int_0^{\infty} x^{z-1} f(x) \mathrm{d}x$. We have that $\mathcal{M}\{\exp(-ax)\}(z) = a^{-z}\Gamma(z)$, for $a > 0, x > 0$, [102], therefore

$$\langle x^q \rangle (s) = \frac{\Gamma(q+1)}{s} \left(p_1 s^{-\alpha_1} + p_2 s^{-\alpha_2} \right)^{q/2}, \quad q = 2, 4, \ldots,$$

which implies the second moment ($q = 2$)

$$\langle x^2 \rangle (t) = 2 \left[\frac{p_1 t^{\alpha_1}}{\Gamma(1 + \alpha_1)} + \frac{p_2 t^{\alpha_2}}{\Gamma(1 + \alpha_2)} \right], \tag{B3}$$

and the fourth-order moment ($q = 4$)

$$\langle x^4 \rangle (t) = 24 \left[\frac{p_1^2 t^{2\alpha_1}}{\Gamma(1 + 2\alpha_1)} + \frac{2 p_1 p_2 t^{\alpha_1 + \alpha_2}}{\Gamma(1 + \alpha_1 + \alpha_2)} + \frac{p_2^2 t^{2\alpha_2}}{\Gamma(1 + 2\alpha_2)} \right]. \tag{B4}$$

B2. 2D PDF

In the two-dimensional case, the qth order moments are given by

$$\langle r^q \rangle (t) = 2\pi \int_0^{\infty} r^{q+1} W^{(2)}(r, t) \mathrm{d}r. \tag{B5}$$

The qth order moment (B5) can be written in the Laplace domain by the aid of equation (44) as

$$\langle r^q \rangle (s) = \frac{1}{s \left(p_1 s^{-\alpha_1} + p_2 s^{-\alpha_2} \right)} \mathcal{M} \left\{ K_0 \left(\frac{r}{\sqrt{p_1 s^{-\alpha_1} + p_2 s^{-\alpha_2}}} \right) \right\} (q+2). \tag{B6}$$

We have that, for $a, r > 0$, $\mathcal{M}\{K_0(ar)\}(z) = 2^{z-2} a^{-z} \left[\Gamma\left(\frac{z}{2}\right) \right]^2$, [102], then

$$\langle r^q \rangle (s) = \frac{2^q \left[\Gamma\left(\frac{q}{2} + 1\right) \right]^2}{s} \left(p_1 s^{-\alpha_1} + p_2 s^{-\alpha_2} \right)^{q/2}, \quad q = 1, 2, \ldots. \tag{B7}$$

Therefore, for even values of q we have

$$\left\langle r^2 \right\rangle (t) = 4 \left[\frac{p_1 t^{\alpha_1}}{\Gamma(1 + \alpha_1)} + \frac{p_2 t^{\alpha_2}}{\Gamma(1 + \alpha_2)} \right], \tag{B8}$$

and the fourth-order moment ($q = 4$)

$$\left\langle r^4 \right\rangle (t) = 64 \left[\frac{p_1^2 t^{2\alpha_1}}{\Gamma(1 + 2\alpha_1)} + \frac{2 p_1 p_2 t^{\alpha_1 + \alpha_2}}{\Gamma(1 + \alpha_1 + \alpha_2)} + \frac{p_2^2 t^{2\alpha_2}}{\Gamma(1 + 2\alpha_2)} \right], \tag{B9}$$

while for the odd values of q, we get the form

$$\left\langle r^q \right\rangle (t) = 2^q \left[\Gamma \left(\frac{q}{2} + 1 \right) \right]^2 (p_1 t^{\alpha_1})^{q/2} E_{\alpha_2 - \alpha_1, \alpha_1 q/2 + 1}^{-q/2}$$
$$\times \left(-\frac{p_2}{p_1} t^{\alpha_2 - \alpha_1} \right), \quad q = 1, 3, \ldots, \tag{B10}$$

where the relation (A17) has been used. The odd qth order moments, (B10), have the asymptotic behaviours, refer to (A15),

$$\left\langle r^q \right\rangle (t) \simeq 2^q \left[\Gamma \left(\frac{q}{2} + 1 \right) \right]^2 \begin{cases} \dfrac{(p_1 t^{\alpha_1})^{\frac{q}{2}}}{\Gamma \left(1 + \frac{\alpha_1 q}{2} \right)}, & t \to 0^+; \\[3mm] \dfrac{(p_2 t^{\alpha_2})^{\frac{q}{2}}}{\Gamma \left(1 + \frac{\alpha_2 q}{2} \right)}, & t \to \infty. \end{cases} \tag{B11}$$

The fact that the $\langle r \rangle (t) \neq 0$ in the radial case is sometimes referred to as 'geometric spurious drift' [103] or 'centrifugal drift' [104].

B3. 3D PDF

In the three-dimensional case, the qth order moments are given in the Laplace domain by

$$\left\langle r^q \right\rangle (s) = \frac{\Gamma (q + 2)}{s} \left(p_1 s^{-\alpha_1} + p_2 s^{-\alpha_2} \right)^{q/2}, \quad q = 1, 2, \ldots. \tag{B12}$$

When $q = 2$, we obtain the second moment

$$\left\langle r^2 \right\rangle (t) = 6 \left[\frac{p_1 t^{\alpha_1}}{\Gamma(1 + \alpha_1)} + \frac{p_2 t^{\alpha_2}}{\Gamma(1 + \alpha_2)} \right], \tag{B13}$$

and when $q = 4$, we get the fourth-order moment

$$\left\langle r^4 \right\rangle (t) = 120 \left[\frac{p_1^2 t^{2\alpha_1}}{\Gamma(1 + 2\alpha_1)} + \frac{2 p_1 p_2 t^{\alpha_1 + \alpha_2}}{\Gamma(1 + \alpha_1 + \alpha_2)} + \frac{p_2^2 t^{2\alpha_2}}{\Gamma(1 + 2\alpha_2)} \right]. \tag{B14}$$

If q is odd, we have the qth order moment

$$\left\langle r^q \right\rangle (t) = \Gamma (q + 2) (p_1 t^{\alpha_1})^{q/2} E_{\alpha_2 - \alpha_1, \alpha_1 q/2 + 1}^{-q/2} \left(-\frac{p_2}{p_1} t^{\alpha_2 - \alpha_1} \right), \quad q = 1, 3, \ldots. \tag{B15}$$

The odd qth order moments $\langle r^q \rangle$ have the asymptotic behaviours:

$$\langle r^q \rangle (t) \simeq \Gamma(q+2) \begin{cases} \dfrac{(p_1 t^{\alpha_1})^{\frac{q}{2}}}{\Gamma\left(1 + \frac{\alpha_1 q}{2}\right)}, & t \to 0^+; \\[3mm] \dfrac{(p_2 t^{\alpha_2})^{\frac{q}{2}}}{\Gamma\left(1 + \frac{\alpha_2 q}{2}\right)}, & t \to \infty. \end{cases} \tag{B16}$$

ORCID iDs

Ralf Metzler ⓘ https://orcid.org/0000-0002-6013-7020

References

[1] Brown R 1828 A brief account of microscopical observations on the particles contained in the pollen of plants and on the general existence of active molecules in organic and inorganic bodies *Phil. Mag.* **4** 161
[2] Einstein A 1905 On the movement of particles suspended in stationary liquids as required by the molecular-kinetic theory of heat *Ann. Phys.* **322** 549
[3] von Smoluchowski M 1906 On the kinetic theory of Brownian molecular movement *Ann. Phys.* **326** 756
[4] Sutherland W 1905 A dynamical theory of diffusion for non-electrolytes and the molecular mass of albumin *Phil. Mag.* **9** 781
[5] Langevin P 1908 On the theory of Brownian motion *C. R. Acad. Sci., Paris* **146** 530
[6] Landau L D and Lifshitz E M 1999 *Physical Kinetics* (Oxford, UK: Butterworth Heinemann)
[7] van Kampen N G 1981 *Stochastic Processes in Physics and Chemistry* (Amsterdam: North-Holland)
[8] Gardiner C 2010 *Stochastic Methods* (Berlin: Springer)
[9] Lévy P 1948 *Stochastic Processes and Brownian Motion* (Paris: Gauthier-Villars)
[10] Øksendal B 2010 *Stochastic Differential Equations: An Introduction with Applications* (Berlin: Springer)
[11] Schilling R L, Song R and Vondracek Z 2012 *Bernstein Functions: Theory and Applications* (Berlin: de Gruyter & Co)
[12] Hughes B D 1995 *Random Walks and Random Environments, Volume 1: Random Walks* (Oxford: Oxford University Press)
[13] Wang B, Kuo J, Bae S C and Granick S 2012 When Brownian diffusion is not Gaussian *Nat. Mater.* **11** 481–5
[14] Chechkin A V, Seno F, Metzler R and Sokolov I M 2017 Brownian yet non-Gaussian diffusion: from superstatistics to subordination of diffusing diffusivities *Phys. Rev. X* **7** 021002
[15] Barkai E and Burov S 2020 Packets of diffusing particles exhibit universal exponential tails *Phys. Rev. Lett.* **124** 060603
[16] Baldovin F, Orlandini E and Seno F 2019 Polymerization induces non-Gaussian diffusion *Front. Phys.* **7** 124
[17] Hapca S, Crawford J W and Young I M 2009 Anomalous diffusion of heterogeneous populations characterized by normal diffusion at the individual level *J. R. Soc. Interface* **6** 111
[18] Cherstvy A G, Nagel O, Beta C and Metzler R 2018 Non-Gaussianity, population heterogeneity, and transient superdiffusion in the spreading dynamics of amoeboid cells *Phys. Chem. Chem. Phys.* **20** 23034
[19] Richardson L F 1926 Atmospheric diffusion shown on a distance-neighbour graph *Proc. R. Soc. A* **110** 709–37
[20] Bouchaud J-P and Georges A 1990 Anomalous diffusion in disordered media: statistical mechanisms, models and physical applications *Phys. Rep.* **195** 127
[21] Metzler R and Klafter J 2000 The random walk's guide to anomalous diffusion: a fractional dynamics approach *Phys. Rep.* **339** 1
[22] Alexander S and Orbach R 1982 Density of states on fractals: fractons *J. Phys. Lett.* **43** 625

[23] Höfling F and Franosch T 2013 Anomalous transport in the crowded world of biological cells *Rep. Prog. Phys.* **76** 046602

[24] Norregaard K, Metzler R, Ritter C, Berg-Sørensen K and Oddershede L 2017 Manipulation and motion of organelles and single molecules in living cells *Chem. Rev.* **117** 4342

[25] Dentz M, Cortis A, Scher H and Berkowitz B 2004 Time behaviour of solute transport in heterogeneous media: transition from anomalous to normal transport *Adv. Water Resour.* **27** 155

[26] Schumer R, Benson D A, Meerschaert M M and Baeumer B 2003 Fractal mobile/immobile solute transport *Water Resour. Res.* **39** 1296

[27] Jeon J-H, Monne H M-S, Javanainen M and Metzler R 2012 Anomalous diffusion of phospholipids and cholesterols in a lipid bilayer and its origins *Phys. Rev. Lett.* **109** 188103

[28] Gupta S, De Mel J U, Perera R M, Zolnierczuk P, Bleuel M, Faraone A and Schneider G J 2018 Dynamics of phospholipid membranes beyond thermal undulations *J. Phys. Chem. Lett.* **9** 2956

[29] Falck E, Róg T, Karttunen M and Vattulainen I 2008 Lateral diffusion in lipid membranes through collective flows *J. Am. Chem. Soc.* **130** 44

[30] Metzler R, Jeon J-H and Cherstvy A G 2016 Non-Brownian diffusion in lipid membranes: experiments and simulations *Biochim. Biophys. Acta Biomembr.* **1858** 2451

[31] Yamamoto E, Kalli A C, Akimoto T, Yasuoka K and Sansom M S P 2015 Anomalous dynamics of a lipid recognition protein on a membrane surface *Sci. Rep.* **5** 18245

[32] Yamamoto E, Akimoto T, Yasui M and Yasuoka K 2014 Origin of subdiffusion of water molecules on cell membrane surfaces *Sci. Rep.* **4** 4720

[33] Toppozini L, Roosen-Runge F, Bewley R I, Dalgliesh R M, Perring T, Seydel T, Glyde H R, Sakai V G and Rheinstädter M C 2015 Anomalous and anisotropic nanoscale diffusion of hydration water molecules in fluid lipid membranes *Soft Matter* **11** 8354

[34] Tan P, Liang Y, Xu Q, Mamontov E, Li J, Xing X and Hong L 2018 Gradual crossover from subdiffusion to normal diffusion: a many-body effect in protein surface water *Phys. Rev. Lett.* **120** 248101

[35] Ghosh S K, Cherstvy A G and Metzler R 2015 Non-universal tracer diffusion in crowded media of non-inert obstacles *Phys. Chem. Chem. Phys.* **17** 1847

[36] Díez Fernández A, Charchar P, Cherstvy A G, Metzler R and Finnis M W 2020 The diffusion of doxorubicin drug molecules in silica nanochannels is non-Gaussian and intermittent *Phys. Chem. Chem. Phys.* **22** 27955

[37] Reverey J F, Jeon J-H, Bao H, Leippe M, Metzler R and Selhuber-Unkel C 2015 Superdiffusion dominates intracellular particle motion in the supercrowded space of pathogenic Acanthamoeba castellanii *Sci. Rep.* **5** 11690

[38] Thapa S, Lukat N, Selhuber-Unkel C, Cherstvy A and Metzler R 2019 Transient superdiffusion of polydisperse vacuoles in highly-motile amoeboid cells *J. Chem. Phys.* **150** 144901

[39] Krapf D *et al* 2019 Spectral content of a single non-Brownian trajectory *Phys. Rev.* X **9** 011019

[40] Ghosh S K, Cherstvy A G, Grebenkov D S and Metzler R 2016 Anomalous, non-Gaussian tracer diffusion in heterogeneously crowded environments *New J. Phys.* **18** 013027

[41] Höfling F, Franosch T and Frey E 2006 Localization transition of the three-dimensional Lorentz model and continuum percolation *Phys. Rev. Lett.* **96** 165901

[42] Bolintineanu D S, Grest G S, Lechman J B and Silbert L E 2015 Diffusion in jammed particle packs *Phys. Rev. Lett.* **115** 088002

[43] Shin J, Cherstvy A G and Metzler R 2015 Self-subdiffusion in solutions of star-shaped crowders: non-monotonic effects of inter-particle interactions *New J. Phys.* **17** 113028
Shin J, Cherstvy A G and Metzler R 2021 *New J. Phys.* **23** 029601 (erratum)

[44] Ambjörnsson T, Lizana L, Lomholt M A and Silbey R J 2008 Single-file dynamics with different diffusion constants *J. Chem. Phys.* **129** 118612

[45] Yamamoto E, Akimoto T, Mitsutake A and Metzler R 2021 Universal relation between instantaneous diffusivity and radius of gyration of proteins in aqueous solution *Phys. Rev. Lett.* **126** 128101

[46] Martin D S, Forstner M B and Käs J A 2002 Apparent subdiffusion inherent to single particle tracking *Biophys. J.* **83** 2109

[47] Monin A S and Yaglom A M 1975 *Statistical Fluid Mechanics: Mechanics of Turbulence* vol 2 ed J L Lumley (Cambridge, MA: MIT Press)

[48] Klafter J, Blumen A and Shlesinger M F 1987 Stochastic pathway to anomalous diffusion *Phys. Rev.* A **35** 3081

[49] Batchelor G K 1952 Diffusion in a field of homogeneous turbulence: II. The relative motion of particles *Math. Proc. Camb. Phil. Soc.* **48** 345

[50] Zaslavsky G M and Niyazov B A 1997 Fractional kinetics and accelerator modes *Phys. Rep.* **283** 73

[51] West B J 2014 Fractional calculus view of complexity: a tutorial *Rev. Mod. Phys.* **86** 1169

[52] Klafter J, Lim S C and Metzler R (ed) 2011 *Fractional Dynamics: Recent Advances* (Singapore: World Scientific)

[53] Klafter J and Sokolov I M 2016 *First Steps in Random Walks* (Oxford: Oxford University Press)

[54] Sandev T and Tomovski Ž 2020 *Fractional Equations and Models: Theory and Applications* (Berlin: Springer)

[55] Evangelista L R and Lenzi E K 2018 *Fractional Diffusion Equations and Anomalous Diffusion* (Cambridge: Cambridge University Press)

[56] Povstenko Y 2016 *Linear Fractional Diffusion-Wave Equation for Scientists and Engineers* (Basel: Birkhäuser)

[57] Schneider W R and Wyss W 1989 Fractional diffusion and wave equations *J. Math. Phys.* **30** 134

[58] Compte A and Metzler R 1997 The generalised Cattaneo equation for the description of anomalous transport processes *J. Phys. A: Math. Gen.* **30** 7277

[59] Caputo M 2001 Distributed order differential equations modelling dielectric induction and diffusion *Fract. Calc. Appl. Anal.* **4** 421

[60] Chechkin A, Gorenflo R and Sokolov I 2002 Retarding subdiffusion and accelerating superdiffusion governed by distributed-order fractional diffusion equations *Phys. Rev.* E **66** 046129

[61] Chechkin A V, Gorenflo R, Sokolov I M and Gonchar V Y 2003 Distributed order time fractional diffusion equation *Fract. Calc. Appl. Anal.* **6** 259

[62] Sokolov I, Chechkin A and Klafter J 2004 Distributed-order fractional kinetics *Acta Phys. Pol.* B **35** 1323

[63] Mainardi F, Pagnini G and Gorenflo R 2007 Some aspects of fractional diffusion equations of single and distributed order *Appl. Math. Comput.* **187** 295

[64] Mainardi F, Mura A, Pagnini G and Gorenflo R 2008 Time-fractional diffusion of distributed order *J. Vib. Control* **14** 1267

[65] Chechkin A, Sokolov I M and Klafter J 2011 Natural and modified forms of distributed-order fractional diffusion equations *Fractional Dynamics: Recent Advances* ed J Klafter, S C Lim and R Metzler (Singapore: World Scientific)

[66] Awad E, Sandev T, Metzler R and Chechkin A 2021 From continuous-time random walks to the fractional Jeffreys equation: solution and applications *Int. J. Heat Mass Transfer* **181** 121839

[67] Awad E, Sandev T, Metzler R and Chechkin A 2021 Closed-form multi-dimensional solutions and asymptotic behaviours for subdiffusive processes with crossovers: I. Retarding case *Chaos Solitons Fractals* **152** 111357

[68] Gorenflo R and Mainardi F 1997 Fractional calculus: integral and differential equations of fractional order *Fract. Fract. Calc. Cont. Mech.* **20** 223

[69] Hilfer R and Anton L 1995 Fractional master equations and fractal time random walks *Phys. Rev.* E **51** R848

[70] Compte A 1996 Stochastic foundations of fractional dynamics *Phys. Rev.* E **53** 4191

[71] Metzler R, Klafter J and Sokolov I M 1998 Anomalous transport in external fields: continuous time random walks and fractional diffusion equations extended *Phys. Rev.* E **58** 1621

[72] Metzler R, Barkai E and Klafter J 1999 Deriving fractional Fokker–Planck equations from a generalised master equation *Europhys. Lett.* **46** 431

[73] Barkai E 2001 Fractional Fokker–Planck equation, solution, and application *Phys. Rev.* E **63** 046118

[74] Barkai E 2002 CTRW pathways to the fractional diffusion equation *Chem. Phys.* **284** 13

[75] Samko S G, Kilbas A A and Marichev O I 1993 *Fractional Integrals and Derivatives: Theory and Applications* vol 1 (London: Gordon and Breach)

[76] Boyadjiev L and Luchko Y 2017 Multi-dimensional α-fractional diffusion-wave equation and some properties of its fundamental solution *Comput. Math. Appl.* **73** 2561

[77] Luchko Y 2017 On some new properties of the fundamental solution to the multi-dimensional space- and time-fractional diffusion-wave equation *Mathematics* **5** 76

[78] Boyadjiev L and Luchko Y 2017 Mellin integral transform approach to analyze the multidimensional diffusion-wave equations *Chaos Solitons Fractals* **102** 127

[79] Langlands T A M 2006 Solution of a modified fractional diffusion equation *Physica* A **367** 136

[80] Awad E and Metzler R 2020 Crossover dynamics from superdiffusion to subdiffusion: models and solutions *Fract. Calc. Appl. Anal.* **23** 55

[81] Klafter J, Blumen A, Shlesinger M F and Zumofen G 1990 Reply to comment on 'Stochastic pathway to anomalous diffusion' *Phys. Rev.* A **41** 1158

[82] Can L, Wei-Hua D and Xiao-Qin S 2014 Exact solutions and their asymptotic behaviours for the averaged generalised fractional elastic models *Commun. Theor. Phys.* **62** 443

[83] Awad E 2020 Dual-phase-lag in the balance: sufficiency bounds for the class of Jeffreys' equations to furnish physical solutions *Int. J. Heat Mass Transfer* **158** 119742

[84] Feller W 1971 *An Introduction to Probability Theory and its Applications* vol 2 (New York: Wiley)

[85] Gorenflo R, Luchko Y and Stojanović M 2013 Fundamental solution of a distributed order time-fractional diffusion-wave equation as probability density *Fract. Calc. Appl. Anal.* **16** 297

[86] Sandev T, Chechkin A V, Korabel N, Kantz H, Sokolov I M and Metzler R 2015 Distributed-order diffusion equations and multifractality: models and solutions *Phys. Rev.* E **92** 042117

[87] Ball R C, Havlin S and Weiss G H 1987 Non-Gaussian random walks *J. Phys. A: Math. Gen.* **20** 4055

[88] Abramowitz M and Stegun I A 1970 *Handbook of Mathematical Functions with Formulas, Graphs, and Mathematical Tables* (Washington, DC: National Bureau of Standards)

[89] Stein E M and Weiss G 1971 *Introduction to Fourier Analysis on Euclidean Spaces* (Princeton, NJ: Princeton University Press)

[90] Porra J M, Masoliver J and Weiss G H 1997 When the telegrapher's equation furnishes a better approximation to the transport equation than the diffusion approximation *Phys. Rev.* E **55** 7771

[91] Mathai A M, Saxena R K and Haubold H J 2010 *The H-Function: Theory and Applications* (Berlin: Springer)

[92] Braaksma B L J 1964 Asymptotic expansions and analytic continuations for a class of Barnes-integrals *Compos. Math.* **15** 239

[93] Prabhakar T R 1971 A singular integral equation with a generalised Mittag Leffler function in the kernel *Yokohama Math. J.* **19** 7

[94] Tomovski Ž, Pogány T K and Srivastava H M 2014 Laplace type integral expressions for a certain three-parameter family of generalised Mittag–Leffler functions with applications involving complete monotonicity *J. Franklin Inst.* **351** 5437

[95] Garra R and Garrappa R 2018 The Prabhakar or three parameter Mittag–Leffler function: theory and application *Commun. Nonlinear Sci. Numer. Simul.* **56** 314

[96] Molina-Garcia D, Sandev T, Safdari H, Pagnini G, Chechkin A and Metzler R 2018 Crossover from anomalous to normal diffusion: truncated power-law noise correlations and applications to dynamics in lipid bilayers *New J. Phys.* **20** 103027

[97] Meerschaert M M and Sabzikar F 2013 Tempered fractional Brownian motion *Stat. Probab. Lett.* **83** 2269

[98] Jeon J-H, Barkai E and Metzler R 2013 Noisy continuous time random walks *J. Chem. Phys.* **139** 121916

[99] Jeon J-H, Tejedor V, Burov S, Barkai E, Selhuber-Unkel C, Berg-Sørensen K, Oddershede L and Metzler R 2011 *In vivo* anomalous diffusion and weak ergodicity breaking of lipid granules *Phys. Rev. Lett.* **106** 048103

[100] Cahoy D O and Polito F 2013 Renewal processes based on generalized Mittag–Leffler waiting times *Commun. Nonlinear Sci. Numer. Simul.* **18** 639

[101] Michelitsch T M and Riascos A P 2020 Continuous time random walk and diffusion with generalized fractional Poisson process *Physica* A **545** 123294

[102] Oberhettinger F 1974 *Tables of Mellin Transforms* (Berlin: Springer)

[103] Godec A and Metzler R 2016 Universal proximity effect in target search kinetics in the few-encounter limit *Phys. Rev.* X **6** 041037

[104] Redner S 2001 *A Guide to First Passage Processes* (Cambridge: Cambridge University Press)